Aus dem Institut für Neuropathologie (Zentrum für Neuropathologie und Prionforschung, ZNP)
der Ludwig-Maximilians-Universität München
Kommissarischer Leiter: Prof. Dr. med. Armin Giese

The role of the Sonic-hedgehog and Wnt/ β-Catenin pathways in medulloblastoma and in embryonal brain tumors with multi-layered rosettes

Dissertation
zum Erwerb des Doktorgrades der Medizin
an der Medizinischen Fakultät der
Ludwig-Maximilians-Universität zu München

vorgelegt von
Edoardo Bianchi
aus
Bozen
Jahr
2016

Mit Genehmigung der medizinischen Fakultät
der Universität München

Berichterstatter: PD Dr. Ulrich Schüller

Mitberichterstatter: Prof. Dr. Rainer Glaß, Priv. Doz. Dr. Nathalie Albert

Mitbetreuung durch den promovierten Mitarbeiter: Dr. Julia Neumann (geb. Pöschl)

Dekan: Prof. Dr. med. dent Reinhard Hickel

Tag der mündlichen Prüfung: 14.04.2016

Major parts of this work have been published as:

Wnt/β-catenin signaling inhibits the Shh pathway and impairs tumor growth in Shh-dependent medulloblastoma.

Pöschl J, Bartels M, Ohli J, Bianchi E, Kuteykin-Teplyakov K, Grammel D, Ahlfeld J, Schüller U.

Acta Neuropathol. 2014;127(4):605-7. doi: 10.1007/s00401-014-1258-2.

Contents

1. Introduction

1.1 The Sonic hedgehog pathway

The Sonic hedgehog (Shh) signalling pathway plays a fundamental role in a multitude of biological processes occurring in embryonic and adult tissues across the metazoa, such as cell proliferation, tissue patterning and cell fate specification (Ingham et al. 2006, Ingham et al. 2011). Its key ligand, the Shh protein, is codified by the *Sonic hedgehog* gene, which belongs to the vertebrate *hedgehog* gene family together with *Desert* and *Indian hedgehog* (Avaron et al. 2006). These three genes are homologous to the Drosophila *hedgehog* gene (*HH*), on which early studies of hedgehog signalling were mainly conducted (Ingham et al. 2011, Robbins et al. 2012). Shh is essential, among others, for patterning and morphogenesis of the embryonic central nervous system (Machold et al. 2002). During neural tube development, the Shh protein is secreted in the notochord and floor plate, hereby playing a central role in the dorso-ventral polarization process of the developing central nervous system (Jessell 2000). The indispensability of hedgehog signalling for the overall brain development has been underlined by studies on morphogenetic pathologies commonly associated with disruption of the Sonic hedgehog pathway, such as holoprosencephaly (Nanni et al. 1999). Holoprosencephaly defines the inability of the prosencephalon to divide itself into the cerebral hemispheres, and mutations of *PTCH1* and *SHH*, which represent key regulators of the hedgehog pathway, have been demonstrated to cause this type of dysmorphology (Nanni et al. 1999). The molecular characterization of the Sonic hedgehog pathway has encountered considerable difficulties, many of which are probably to ascribe to the hydrophobic nature of the Sonic hedgehog protein (Mann et al. 2004). Shh is translated as a 45 kDa precursor protein, which is than cleaved auto-catalytically into two peptides before secretion (Bumcrot et al. 1995), whereas the Shh-N (amino-terminal) peptide acts as the proper Shh-signalling activator (Hammerschmidt et al. 1997). The Shh protein binds to the heterodimeric Patched-Smoothened receptor complex, therefore initiating Shh signalling activation **(Figure 1)**. If Shh is absent, Patched (Ptch) represses the activity of Smoothened (Smo), a transmembrane protein, which belongs to the Frizzled family of receptors, thus inactivating the Sonic hedgehog pathway (Taipale et al. 2002). Upon binding of Shh to Patched, the Sonic hedgehog pathway is activated through Smoothened disinhibition (Ingham et al. 1991). In vertebrates, the glioma-associated oncogene family zinc finger proteins (Gli) are the ultimate effectors in the transduction of Sonic hedgehog signalling (Ingham et al. 2001), whereas the molecular mechanisms involved in the modulation of

the Gli transcription factors remain poorly understood (Ingham et al. 2011). Gli1 displays exclusively activating properties on the transcription of Shh target genes (Bai et al. 2004). Gli2 and Gli3, on the other hand, present a double molecular function. Their full-length forms act as transcriptional activators under the control of Smoothened, but also give rise, in absence of Shh, to repressive Gli forms after removal of specific C-terminal domains (Sasaki et al. 1999, Robbins et al. 2012).

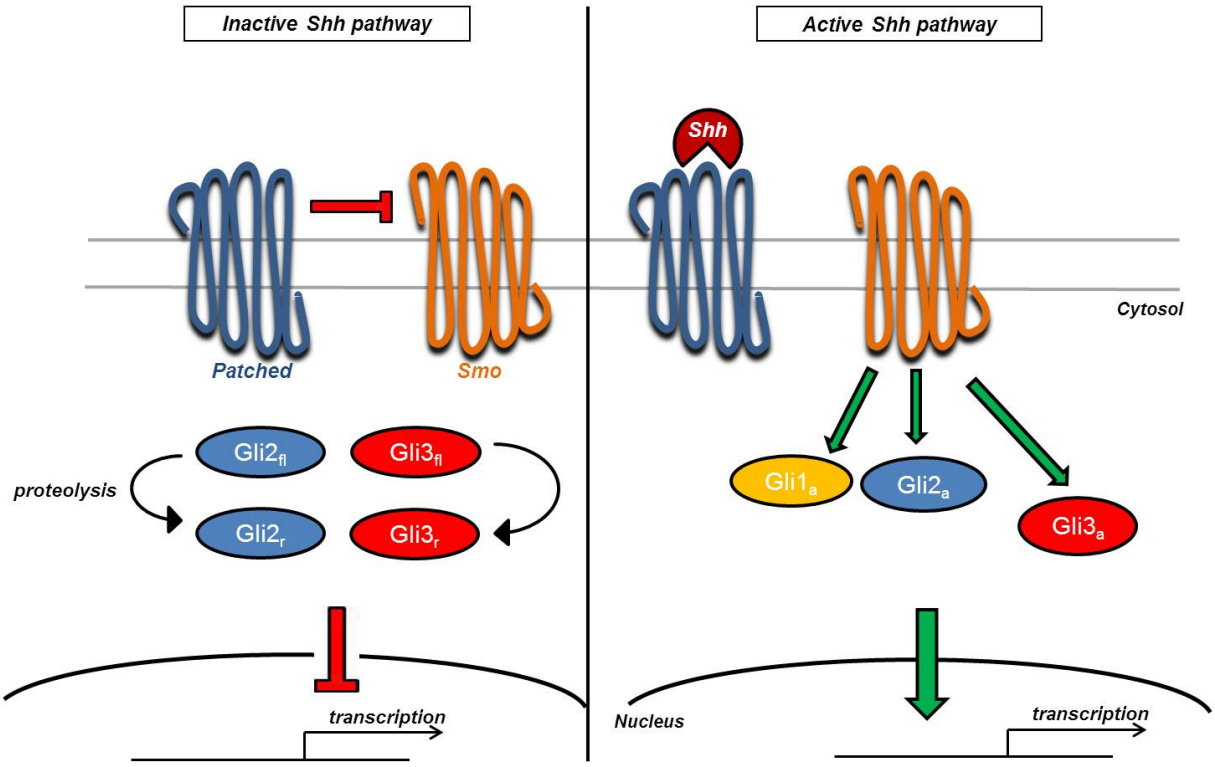

Figure 1. The Sonic hedgehog pathway. In absence of Sonic hedgehog (Shh), Patched inhibits Smoothened therefore inactivating Sonic hedgehog signalling. The binding of Shh to the Patched receptor leads to a conformational change and disinhibition of Smoothened. On its behalf, Smoothened induces the activation of the Gli transcription factors (Gli_a), whereas the molecular interaction between Smo and Gli remains poorly understood, especially in vertebrates (Robbins et al. 2012 for review). Gli1 acts exclusively as a transcriptional activator. Gli2 and Gli3, on contrary, present an activating full-length (Gli_{fl}) as well as a repressive form (Gli_r), the latter of which is generated through post-translational modification of the Gli1 and Gli2 proteins in absence of Shh.

In the cerebellum, Shh is fundamental for the proliferation of cerebellar granule neuron precursor cells (CGNPs) in the external granule layer (Wechsler-Reya et al. 1999) and persistent Shh activation is able to drive the formation of a particular, Shh-dependent medulloblastoma subgroup (Pietsch et al. 1997, Northcott et al. 2012). Furthermore, dysregulation of the Shh pathway plays a role in the induction of tumors occurring in different human tissues, such as Basal cell carcinoma (Athar et al. 2014) or Pancreatic

ductal carcinoma (Lauth et al. 2011). Molecules targeting different components of the Sonic hedgehog pathway, such as the Smoothened inhibitor Vismodegib, have already been subject of clinical trials aiming at the consolidation of novel therapeutic approaches against Shh-driven neoplastic pathologies (Sekulic et al. 2012).

1.2 The Wnt pathway

The Wnt (Wingless related integration site) pathway is a highly conserved signalling pathway, which was first discovered due to its role in carcinogenesis (Nusse et al. 1982) and body axis formation during embryonic development (Klaus et al. 2008). Up until now, three different Wnt-associated pathways have been identified: the canonical Wnt pathway (also called Wnt/ β-Catenin pathway), the non-canonical planar cell polarity (PCP) pathway and the non-canonical Wnt/ calcium pathway (Komiya et al. 2008). As far as molecular mechanisms and biological implications are concerned, the Wnt/ β-Catenin pathway remains better understood than the non-canonical Wnt pathways (Freese et al. 2010). Mutational analysis of Wnt-related genes was able to elucidate the importance of Wnt for a wide range of developmental processes (Logan et al. 2004 for review), including, among others, gastrulation (Barrow et al. 2003) or anterior-posterior body axis extension (Yamaguchi et al. 1999). In the central nervous system, canonical Wnt signalling is fundamental for forebrain development (Kim et al. 2000, Freese et al. 2010) in a dose- and gradient-dependent manner (Popperl et al. 1997). With particular regard to embryonic and postnatal cortical development, Wnt/ β-Catenin signalling has been shown to regulate the proliferation of neuronal cortical progenitor cells of the ventricular zone as well as neuronal lineage choice (Chenn et al. 2002, Backman et al. 2005, Pöschl et al. 2013). In cerebellar development, the importance of Wnt/ β-Catenin has been underlined by studies showing that constitutional Wnt/ β-Catenin activation leads to an overall disruption of the cerebellar histological architecture and impaired proliferation of granule neuron precursor cells (Lorenz et al. 2011, Pöschl et al. 2013). In particular, a time-dependent Wnt/ β-Catenin activation or downregulation as well as the interplay with the Sonic hedgehog pathway appear to be fundamental for normal cerebellar development (Selvadurai et al. 2011, Pöschl et al. 2013). In canonical Wnt signalling (Clevers et al 2012 for review), Wnt proteins bind to an heterodimeric receptor complex **(Figure 2)** consisting of the 7-transmembrane Frizzled receptor (Fz) (Janda et al. 2012) and the LRP5/6 protein (Pinson et al. 2000). The following transduction of the Wnt signal through β-Catenin stabilization is regulated by the cytoplasmic destruction complex, which com-

prises Axin, Adenomatous polyposis coli (APC), Dishevelled (Dvl), CK1 and GSK3 (Aberle et al. 1997, Clevers et al. 2012). In the absence of Wnt, Axin binds β-Catenin and the serine/ threonine kinases CK1 (α/δ) and GSK3 (α/β) subsequently phosphorylate β-Catenin leading to its ubiquitination and proteasomal degradation (Aberle et al. 1997, Clevers et al. 2012). Wnt proteins, on the other hand, induce a conformational change of the Frizzled/LRP receptor complex followed by phosphorylation of LRP6, which is necessary for Axin-LRP6 binding and therefore for the disruption of the cytoplasmic destruction complex (Tamai et al. 2004). As a consequence, β-Catenin is stabilized and shifted to the nucleus, where it interacts with transcription factors of the TCF/LEF family, ultimately leading to Wnt target genes expression (Behrens et al. 1996).

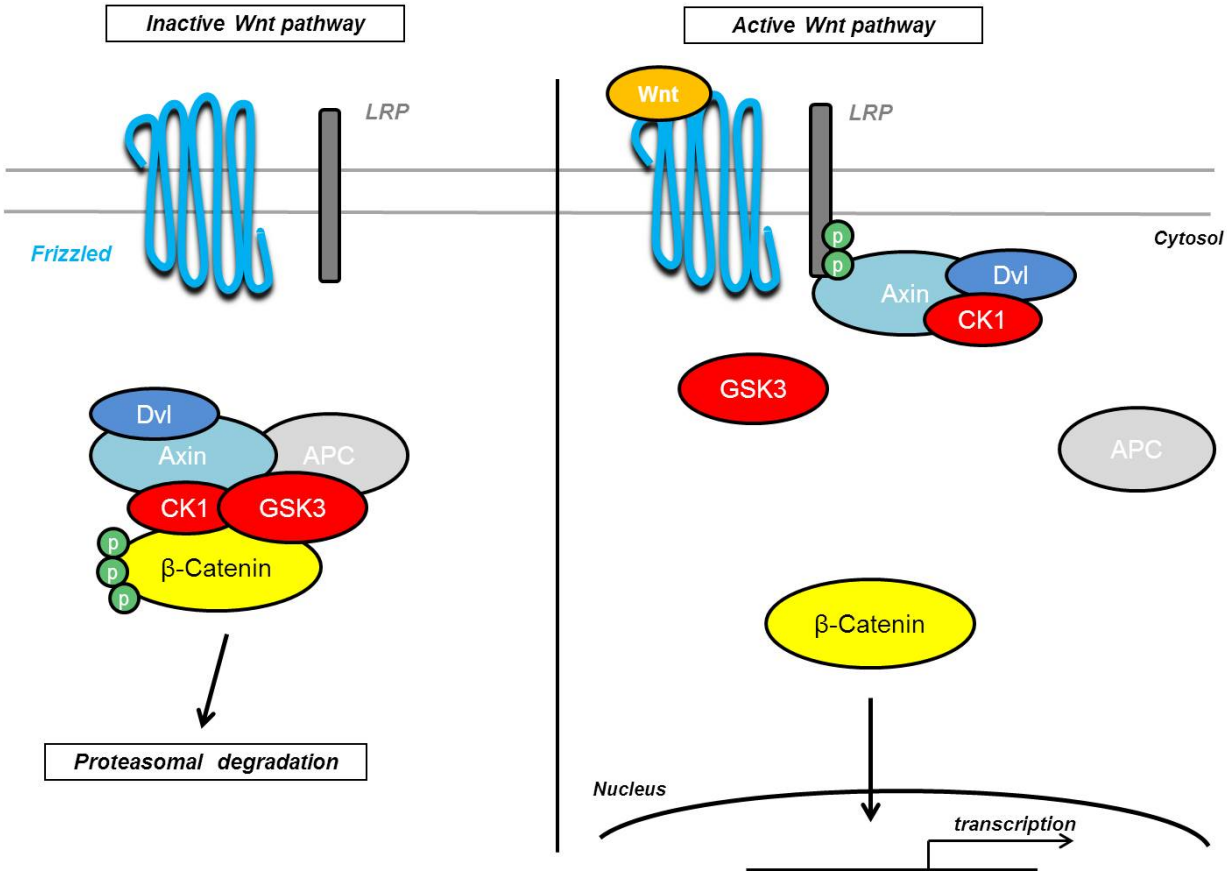

Figure 2. The Wnt/ β-Catenin pathway. In the absence of Wnt, β-Catenin is phosphorylated by Glycogen Synthase Kinase 3 (GSK3) and the CK1-kinase group, which are part of the cytoplasmic destruction complex, together with Dishevelled (Dvl), Axin and Adenomatous Polyposis Coli (APC). After phosphorylation and subsequent ubiquitination, β-Catenin is inactivated through proteasomal degradation. If present, Wnt binds the heterodimeric Frizzled-LRP5/6 receptor, which undergoes a conformational transformation. As a result, Axin binds to phosphorylated LRP5/6, thus disrupting the cytoplasmic destruction complex. Consequently, β-Catenin is stabilized and shifted to the nucleus (Clevers et al. 2006 for review).

The Wnt/ β-Catenin pathway has been demonstrated to play an essential role in the regulation of stem cell renewal, cell differentiation (Korinek et al. 1997, Ten Berge et al. 2011) and ultimately- oncogenesis (Klaus et al. 2008). *APC* mutations, for instance, are

associated with Familiary Adenomatous Polyposis (FAP) as well as sporadic colorectal cancer (Kinzler et al. 1991, Kinzler et al. 1996). With regard to CNS malignancies, a particular subgroup of medulloblastoma arising from the dorsal brainstem might be driven by Wnt activation (Gibson et al. 2010) and simultaneous Shh and Wnt activation may characterize Embryonal tumors with multi-layered rosettes (ETMRs), a subset of CNS-PNETs (Korshunov et al. 2012, Picard et al. 2012).

1.3 Embryonal brain tumors

Embryonal brain tumors are the largest group of malignant CNS tumors in children, often presenting as poorly differentiated, highly malignant neoplasms with small, round cells and high cellularity (Grech-Sollars et al. 2012, Sin-Chan et al. 2014, Wesseling 2014). Medulloblastoma, Primitive neuroectodermal tumors of the CNS (CNS-PNETs) and Atypical teratoid/ rhabdoid tumors (AT/RTs) are typical members of this tumor group **(Figure 3)**.

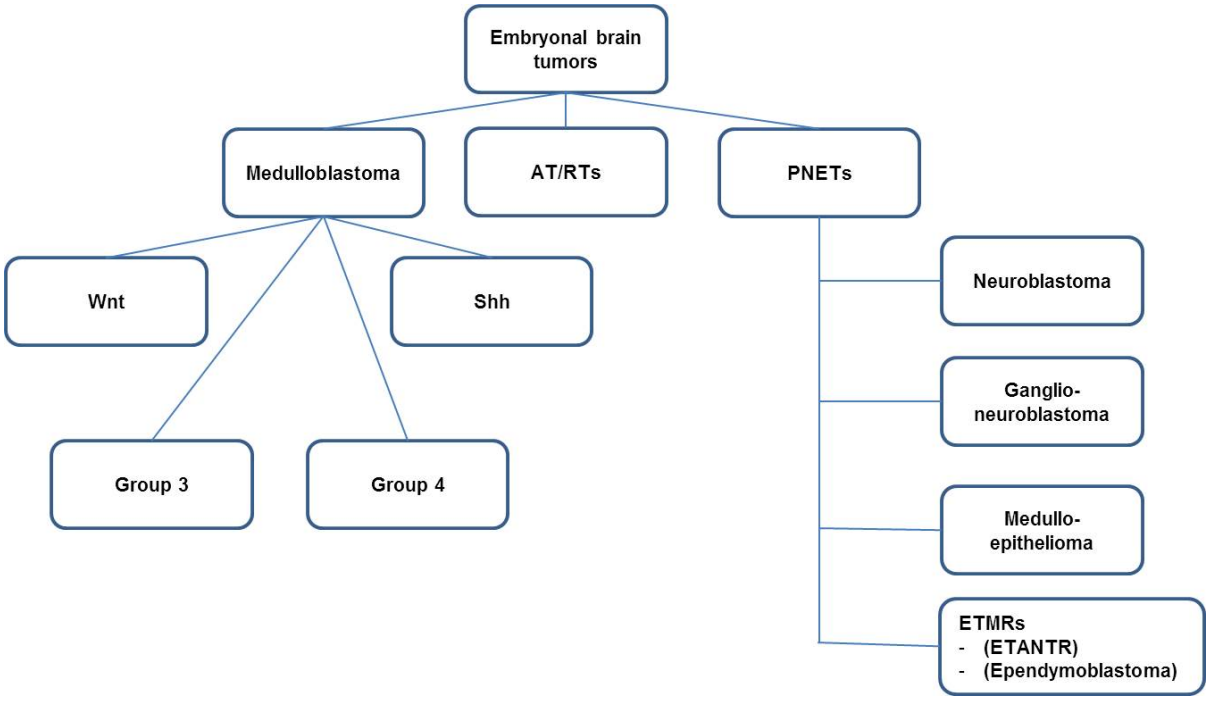

Figure 3. Embryonal brain tumors. Taylor et al. were the first to delineate a molecular classification of medulloblastoma into four groups; namely Wnt, Sonic hedgehog, Group 3 and Group 4. As far as CNS-PNETs are concerned, the 2007 WHO Classification of Tumours of the Central Nervous System defines the following histological subcategories: Neuroblastoma, Ganglioneuroblastoma, Medulloepithelioma and Ependymoblastoma. More recently, a new PNET subset called „ETANTR“ (embryonal tumor with abundant neurop il and true rosettes) was delineated (Gessi et al. 2009). Following increasing evidence that Ependymoblastomas, Medulloepitheliomas and ETANTRs probably represent a single tumor entity, in 2010 Paulus and Kleihues coined the term ETMR (Embryonal tumor with multilayered rosettes), which regroups these types of tumors.

Medulloblastoma

Medulloblastoma is the most common malignant brain tumor of the childhood (Remke et al. 2013). The incidence of medulloblastoma in the USA resides around 9.6 per million for pediatric cases and 0.54 per million for adult cases (Thorne et al. 1994, Giordana et al. 1999), with other countries displaying similar incidence (Gjerris et al. 1998). The clinical manifestation of medulloblastoma often comprises symptoms typically associated with increased intracranial pressure, such as nausea/vomiting or headaches, as well as cerebellar signs like ataxia or oculomotoric disorders (Alston et al. 2003). Metastatic dissemination through cerebral fluid in the craniospinal axis is a major prognostic factor and challenging clinical aspect in the treatment of medulloblastoma (Gajjar et al. 2006, Wu et al. 2012). The 5-year survival rate ranges between 65% for high-risk disease and 89% for average risk disease (Remke et al. 2013), with the adult cases presenting a worse prognosis (Smoll 2012). The 2007 WHO classification of brain tumors, based on which medulloblastoma is diagnosed in clinical practice, includes five histological subtypes: classic, desmoplastic/nodular, large-cell, anaplastic and medulloblastoma with extensive nodularity (Louis et al. 2007). All histological subtypes are classified as WHO grade IV tumors, representing the highest grade of malignancy (Louis et al. 2007). A further subdivision of medulloblastoma in four molecular groups, namely Shh-induced, Wnt-induced, Group 3 and Group 4 tumors **(Figure 3)**, has recently been delineated (Northcott et al. 2012). Besides array-based expression patterns, the cellular origin of medulloblastoma subgroups has been subject of recent investigations. Shh-associated medulloblastoma appears to arise from cerebellar granule neuron precursors (GNPs) (Schüller et al. 2008) or cochlear granule neuron precursors (Grammel et al. 2012), whereas Wnt-induced medulloblastoma might take origin from dorsal brainstem precursor cells (Gibson et al. 2010). The current therapeutic approach for medulloblastoma is multimodal, consisting of a combination of surgical resection, radiation of the tumor site and the craniospinal axis, and chemotherapy (Roussel et al. 2011). Neurological dysfunctions and cognitive impairment are the main side effects of this course of therapy (Ris et al. 2001), giving rise to the need for specific, targeted therapies. Based on the newly discovered molecular clustering of medulloblastoma, some subgroup specific therapies, especially for the Shh-dependent group, have already been matter of experimental studies (Taipale et al. 2000) and clinical trials (Rudin et al. 2009).

Embyonal tumors with multi-layered rosettes

CNS-PNETs, previously known as supratentorial PNETs, make up about 3-5% of all pediatric brain tumors (Picard et al. 2012). These tumors mainly originate in the cerebral hemispheres and typically feature a variable histological presentation, including either poor differentiation or neuronal, ependymal and glial elements (Louis et al. 2007). Similarly to medulloblastoma, CNS-PNETs often show the tendency to disseminate in the leptomeningeal space (Pizer et al. 2006). The current therapy protocols for CNS-PNETs, which resemble standard medulloblastoma treatment (Pizer et al. 2006), are associated with a poor prognosis not reaching 50% of survival after 3 years (Timmermann et al. 2006). For this reason new and specific therapeutic approaches for CNS-PNETs are highly desirable. In comparison to medulloblastoma, for which an array-based molecular characterization has been carried out (Northcott et al. 2012), the molecular and cellular underpinnings of CNS-PNETs remain widely unknown (Li et al. 2005). According to the 2007 WHO classification of brain tumors **(Figure 3)**, CNS-PNETs are divided into four histological groups: neuroblastomas, ganglioneuroblastomas, medulloepitheliomas and ependymoblastomas (Louis et al. 2007), whereas a particular subset of CNS-PNETs presents multi-layered rosettes on histological assessment (Korshunov et al. 2010). The diagnostic classification of this particular tumor entity was poorly defined in the past (Wesseling 2014), leading to divergent definitions, such as ependymoblastoma, or –recently- ETANTR (Embryonal tumor with abundant neuropil and rosettes) (Korshunov et al. 2010). Li et al. were the first to discover the amplification of a chromosome 19q13.41 miRNA polycistron (C19mC) as a common feature within a particular subgroup of PNETs with “ependymoblastic” histological features (Li et al. 2009), thus delineating a new diagnostic entity comprising the formerly applied terms of ependymoblastoma, medulloepithelioma, and ETANTR, namely ETMRs (Embryonal tumors with multi-layered rosettes) (Korshunov et al. 2010, Eberhart 2011).

1.4 Interaction of Shh and Wnt/ β-Catenin in embryonal brain tumors

A possible interaction between the Shh and Wnt pathway in the central nervous system, particularly in terms of an antagonistic role of Wnt over Shh activation, has been matter of study in recent years (Yu et al. 2008, Tang et al. 2010). The hypothetical inhibitory effect of Wnt on Shh might be corroborated by findings showing that Wnt is able to antagonize Shh during neural tube patterning (Alvarez-Medina et al. 2008). In the cerebellum, constitutional activation of Wnt was demonstrated to be able to down-regulate the

Shh pathway and inhibit the Shh-driven proliferation of cerebellar granule neuron precursor cells as well as Shh-dependent medulloblastoma tumor growth in mice (Lorenz et al. 2011, Pöschl et al. 2014). Hence, the antagonizing effect of Wnt over Shh should be further investigated with respect to a possible use of Wnt-activating substances, such as Lithium (Lancaster et al. 2011), in the therapy of Shh-driven medulloblastoma. Interestingly, recent array-based studies on CNS-PNETs identified a molecular tumor cluster, called “group 1” PNET, which displayed both Wnt and Shh upregulation (Picard et al. 2012). Both “group 1” PNETs and the newly defined EMTRs appeared to be characterized by frequent C19mC amplification and overexpression of the molecular marker *LIN28* (Korshunov et al. 2012, Picard et al. 2012), which suggests that EMTRs and “Group 1” PNETs might actually represent the same pathological entity. Hence, it is possible to propose the hypothesis that the observed inhibitory effect of Wnt over Shh in the cerebellum might be spatially-related and not applicable to other regions of the central nervous system, such as the forebrain. On the contrary, a possible synergistic and tumor-inducing role of simultaneously activated Wnt and Shh in EMTR formation should be subject of further research.

1.5 Aim of this study

This work intends to investigate the diverging role of synchronistic Wnt and Shh activation in Shh-dependent medulloblastoma and Embryonal tumors with multi-layered rosettes, with particular regard to a possible therapeutic approach. A series of *in vitro* and *in vivo* experiments was carried out, aiming at the possible use of Lithium, a Wnt activator, in the therapy of Shh-driven medulloblastoma. Furthermore, the first conditional mouse model for Embryonal tumors with multi-layered rosettes (ETMR) was established and a possible role of Wnt and Shh upregulation in ETMR formation has been postulated.

2. Material and methods

2.1 Transgenic mice

Math1-cre mice

Math1-cre mice are transgenic mice, which carry a P1 bacteriophage Cre recombinase sequence under the control of a 1.4-kb upstream *Math1* (also called: *Atoh1*) promotor. This results in a specific expression of Cre recombinase in *Math1*-expressing granule

neuron precursors (GNPs) of the cerebellum (Matei et al. 2005, Schüller et al. 2007). The following primers were used to detect the presence of the *Math1-cre* construct:

Cre Fw	5´- TCCGGGCTGCCACGACCAA - 3´
Cre Rv	5´- GGCGCGGCAACACCATTTT - 3´
From Heine et al. 2009, annealing temperature: 65 °C	

SmoM2$^{Fl/FL}$ mice

SmoM2$^{Fl/Fl}$ mice bear a modified gene sequence of the Smoothened (Smo) transmembrane protein, which is a key regulator in Sonic Hedgehog signalling (see introduction, Figure 1). The W539L point mutation of the *Smoothened* gene, defined as *SmoM2* mutation, leads to autonomous Smoothened activation and therefore to constitutional Sonic hedgehog activation (Xie et al. 1998, Mao et al. 2006). A polyadenilation (4xpA) stop sequence upstream of *SmoM2* is flanked by two loxP sites. In presence of Cre recombinase, the 4xpA stop sequence is excised. This results in uninhibited *SmoM2* transcription and therefore Shh activation **(Figure 4)**.

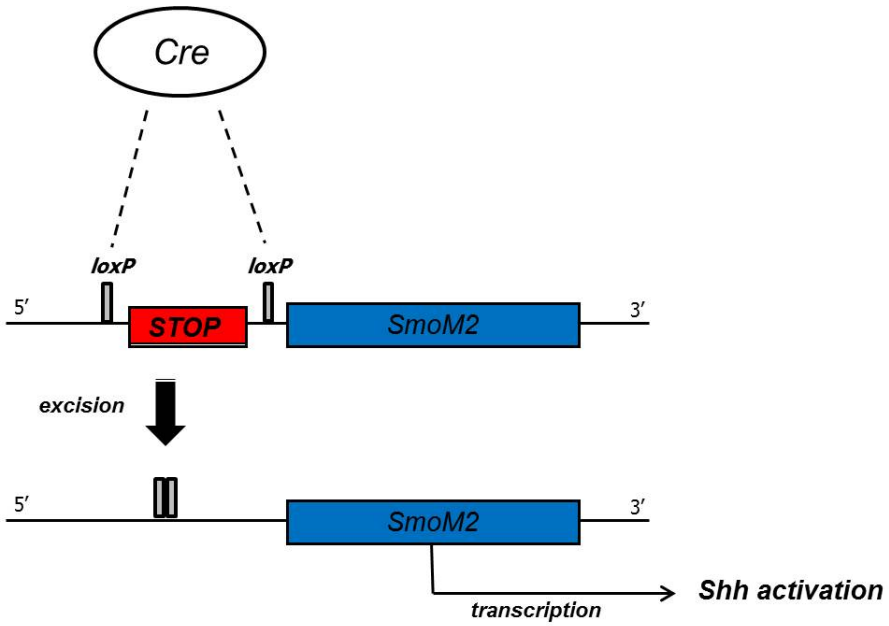

Figure 4. The *SmoM2$^{Fl/Fl}$* transgenic construct. The *SmoM2* mutation of the *Smoothened* (*Smo*) gene is preceded by an upstream, loxP-flanked stop sequence (polyadenilation sequence, 4xpA). In presence of Cre recombinase, the stop sequence is excised, leading to *SmoM2* transcription and therefore Sonic hedgehog activation.

The following Primers were used to detect the presence of the *SmoM2*$^{Fl/Fl}$ allele:

SmoM2 Fw	5´- AAGTTCATCTGCACCACCG - 3´
SmoM2 Rv	5´- TCCTTGAAGAAGATGGTGCG - 3´
From Jeong et al. 2004, annealing temperature: 60 °C	

In order to achieve constitutional Shh activation in *Math1*-positive cells, *Math1-cre* and *SmoM2*$^{Fl/Fl}$ mice were bred **(Figure 5)** and *Math1-cre::SmoM2*$^{Fl/+}$ mice were generated (Schüller et al. 2008).

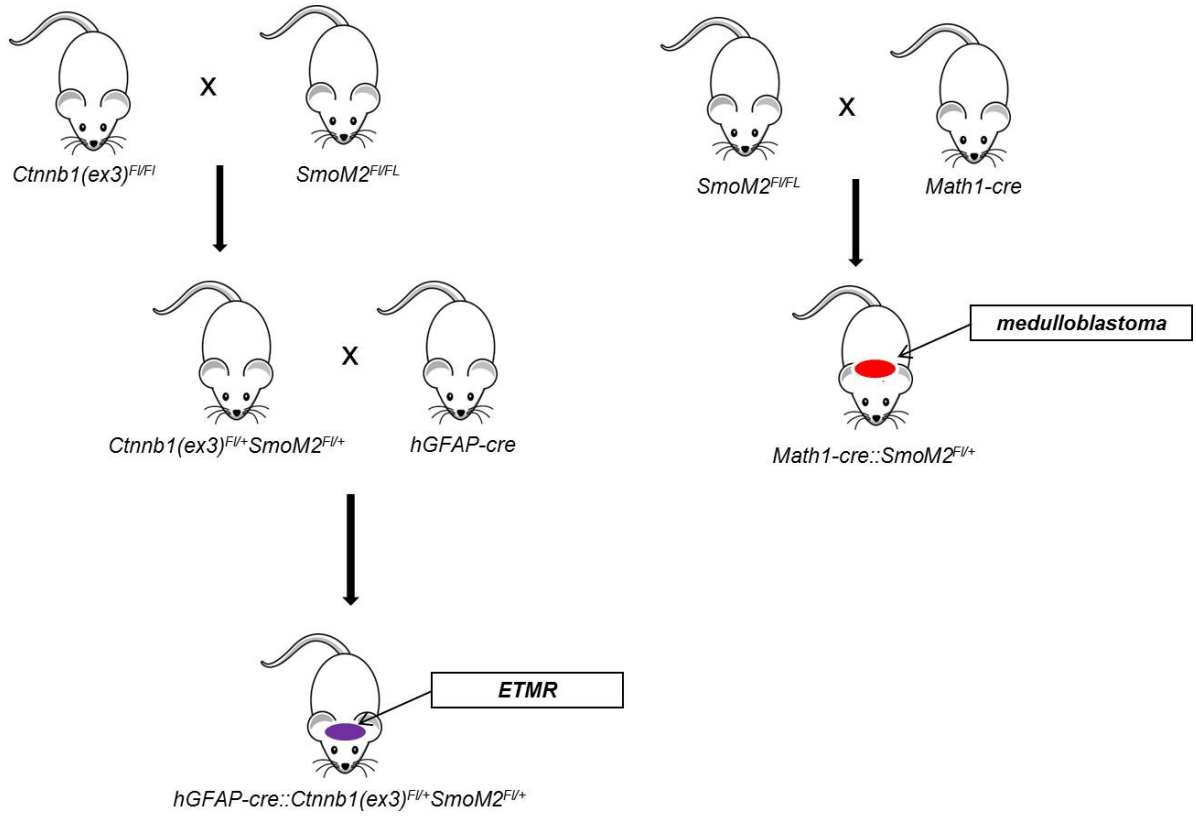

Figure 5. Breeding scheme for generating *Math1-cre::SmoM2*$^{Fl/+}$ *and hGFAP-cre::Ctnnb1(ex3)*$^{Fl/+}$ *SmoM2*$^{Fl/+}$ *mice*

Ctnnb1(ex3)$^{Fl/Fl}$ *mice*

Ctnnb1(ex3)$^{Fl/Fl}$ mice (Harada et al. 1999, Pöschl et al. 2013) are characterized by the presence of a modified *β-Catenin* (*Ctnnb1*) gene sequence, which consists of two loxP sites flanking Exon 3 (ex3) **(Figure 6)**. Exon 3 codifies particular domains of the β-Catenin protein, which include Glycogen synthase kinase 3 beta (GSKβ) phosphorylation sites. Through Cre-mediated recombination Exon 3 is excised, resulting in a trun-

cated β-Catenin without phosphorylation sites but still intact ability to act as a transcription factor (Harada et al. 1999). This leads to a stabilized β-Catenin and consequently Wnt activation (Barth et al. 1997).

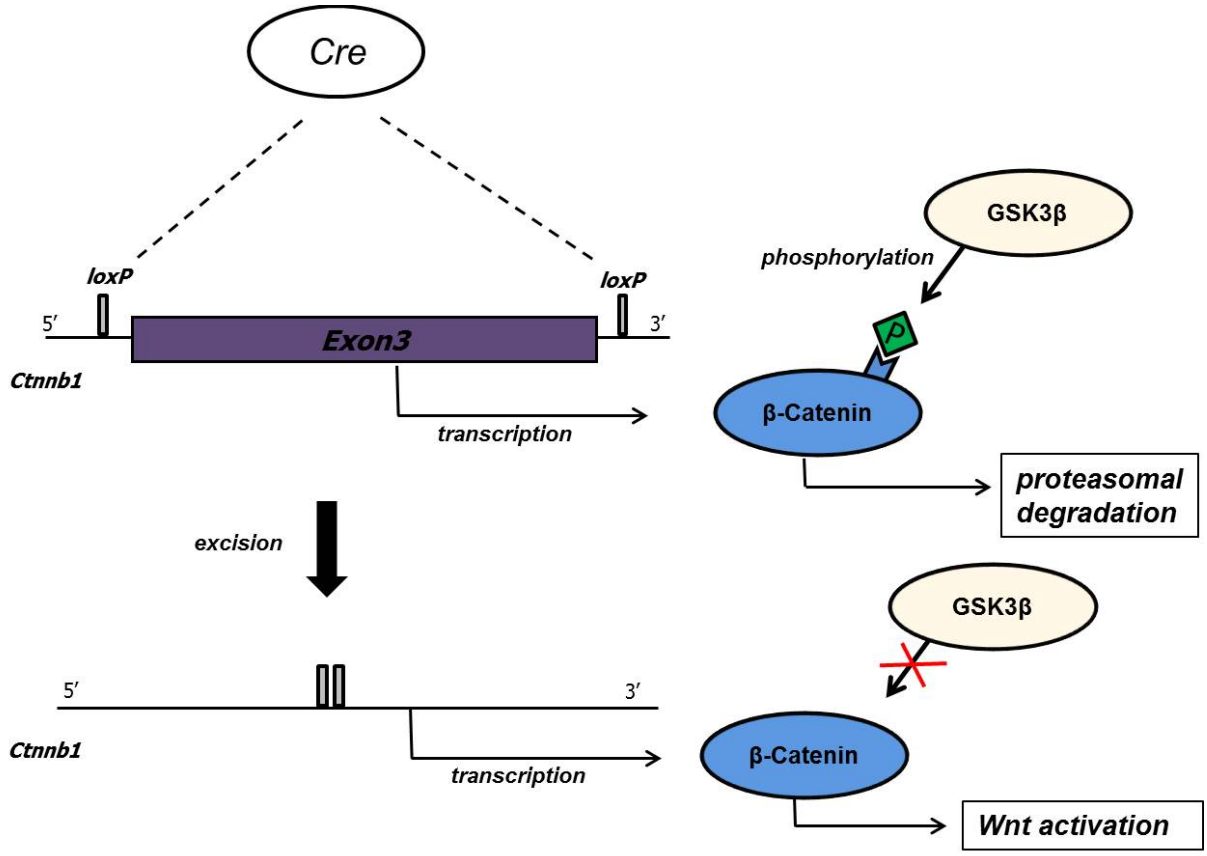

Figure 6. The *Ctnnb1(ex3)*$^{Fl/Fl}$ transgene. Exon 3 of the *β-Catenin* (*Ctnnb1*) gene is located between two loxP sequences. Exon 3 codifies domains of the β-Catenin protein, which serve as phosphorylation sites for Glycogen synthase kinase 3 beta (GSK3B). When Cre recombinase is expressed, Exon 3 is removed leading to β-Catenin stabilization through missing phosphorylation and therefore Wnt/ β-Catenin activation.

The following Primers were used to detect the presence of the *Ctnnb1(ex3)*$^{Fl/Fl}$ allele:

Ctnnb1(ex3)$^{Fl/Fl}$ Fw	5´- CGTGGACAATGGCTACTCAA - 3´
Ctnnb1(ex3)$^{Fl/Fl}$ Rv	5´- TGTCCAACTCCATCAGGTCA - 3´
Annealing temperature: 60 °C	

hGFAP-cre mice

hGFAP-cre mice express Cre recombinase under the control of an upstream enhancing sequence, which consists of the promotor of *human glial fibrillary acidic protein* (*hGFAP)*. The *hGFAP* promotor targets a wide range of cell populations of the brain, including neural precursors and glial cells (Zhuo et al. 2001). After generating

Ctnnb1(ex3)$^{Fl/Fl}$SmoM2$^{Fl/Fl}$ mice, *hGFAP-cre* and *Ctnnb1(ex3)$^{Fl/Fl}$SmoM2$^{Fl/Fl}$* mice were crossed **(Figure 5)**. The newly developed *hGFAP-cre::Ctnnb1(ex3)$^{Fl/+}$SmoM2$^{Fl/+}$* mice enabled the achievement of a synchronistic activation of both Shh and Wnt/β-Catenin in the *hGFAP*-positive cell population. The following Primers were used to detect the presence of the *hGFAP*-cre allele:

hGFAP Fw	5´- ACTCCTTCATAAAGCCCTCG - 3´
hGFAP Rv	5´- ATCACTCGTTGCATCGACCG - 3´
From Zhuo et al. 2001, annealing temperature: 65 ºC	

Ptch1$^{+/-}$ mice

Ptch1 is a key regulator of Sonic hedgehog signalling (see Figure 1). *Ptch1$^{+/-}$* mice (Goodrich et al. 1997) are a Shh-dependent medulloblastoma mouse model carrying a knocked-out *Ptch1* allele **(Figure 7)**, which is achieved as a result of homologous recombination: part of Exon 1 and all of Exon 2 of the *Ptch1* gene are replaced by a construct containing *lacZ*, a commonly used reporter gene (Juers et al. 2012), and a neomycin resistance gene (Goodrich et al. 1997). Upon random loss of the wild-type *Ptch1* allele, *Ptch1$^{+/-}$* mice eventually develop medulloblastoma. This occurs in about 15-20% of the *Ptch1$^{+/-}$* mice (Oliver et al. 2005). The following Primers were used to detect the presence of the mutated *Ptch1* allele:

Ptch1 Fw	5´- GCCCTGAATGACTGCAGGACG - 3´
Ptch1 Rv	5´- CACGGGTAGCCAACGCTATGTC - 3´
Annealing temperature: 65 ºC	

NMRI-Nu/Nu mice

NMRI-Nu/Nu mice are nude mice characterized by hairless skin from birth as well as thymus dysgenesis with subsequent T-lymphocytes depletion (Pantelouris et al. 1970, Pignata et al. 1996, Schlake 2001). A homozygote mutation of the *FoxN1* (*Forkhead box N1*) gene, which is located on chromosome 11 in mice, is responsible for this particular phenotype (Nehls et al. 1994, Schorpp et al. 1997). Nude mice are a well-established murine model for immunological, oncological and transplantation studies due to their lack of competent T-lymphocytes (Zhang et al. 2012).

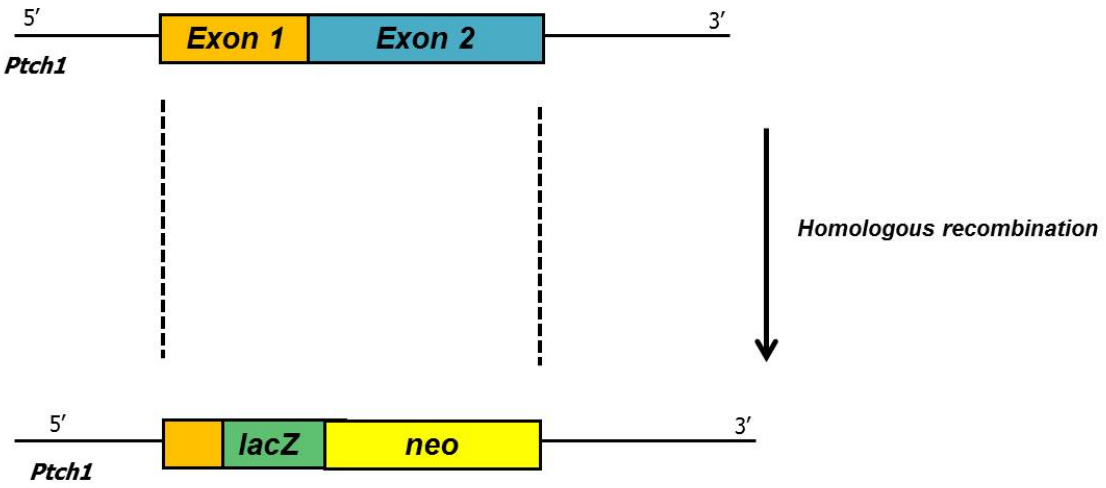

Figure 7. The *Ptch1*$^{+/-}$ knockout transgene. Part of Exon 1 and all of Exon 2 of the *Ptch1* gene are replaced through homologous recombination by a gene cassette containing a *lacZ* marker sequence and a neomycin resistance gene, thus resulting in *Ptch1* knockout.

2.2 DNA extraction

DNA for genotype verification through PCR and electrophoresis was extracted from mouse tail biopsies. Each biopsy was first treated with 500 µl Laird´s lyses buffer (200 mM NaCl, 100 mM Tris buffer (pH 8.5), 5 mM EDTA, 0.2% SDS) and 10 µl Proteinase K (10mg/ml) on a thermo-shaker at 56ºC for at least 2 hours. Samples were than centrifuged (14.000 U) at room temperature for 5 minutes. The supernatant containing the DNA was then extracted into a new tube and 500 µl Isopropanol were added. After mixing, the precipitated DNA became visible. Centrifugation at room temperature with 14.000 U for 5 minutes was repeated. Finally, the remaining Isopropanol was discarded and the DNA pellet was re-suspended in DEPC water and then stored at 4ºC.

2.3 Cell lines

HEK 293T, UW473 and GL261

HEK 293T cells arise from human embryonic kidney cells, which were originally transformed with Adenovirus 5 DNA (Graham et al. 1977). UW473 is a human medulloblastoma cell line obtained from a pediatric tumor sample (Bobola et al. 2005, Castro-Gamero et al. 2013). GL261 cells derive from the GL261 mouse glioma model. This murine model was first developed through application of a chemical carcinogen into the brain of C57BL/6 mice and then perpetuated by means of syngeneic transplantation (Maes et al. 2011). All three cell lines proliferated as adherent monolayers and were cul-

tured in DMEM medium with 10% fetal calf serum, 1% Glutamax (Invitrogen), 1% Penicillin/Streptomycin (Invitrogen) and 1% HEPES buffer (Sigma).

2.4 Primary cell culture

Cerebellar granule neuron precursor cells

Well plates were coated with 1x poly-L-ornithine (Sigma) from a 100x stock (10 mg/ml). Dilution was carried out in H_2O and 0.2 µM sterile filters were used in order to preserve poly-L-ornithine. The plates were than incubated at 37ºC during mouse preparation allowing poly-ornithine to polymerise. Mouse cerebella were dissected at postnatal day 5-7 and put on ice in 15 ml Hanks buffered saline solution (Gibco, pH 7.4 Glucose 6 mg/L). After centrifugation at 4ºC for 5 minutes with 800 rpm, HBSS was discarded. 1 ml of 1x Trypsin/EDTA/DNAse (100 µg DNAse/ml, both Trypsin/EDTA and DNAse were from Sigma) was added and the cerebella were left 10 minutes in water bath for incubation. Trypsin was then inactivated with 2 ml of DMEM+10% fetal bovine serum (fetal bovine serum was inactivated at 56ºC for 30 minutes prior to usage). Next, the cerebella were centrifuged at 4ºC with 1500 G for 5 minutes. The fetal bovine serum medium was aspirated and substituted with 5 ml HBSS solution. The pellets were dissolved by pipetting gently and a new centrifugation step (as above) was conducted. After discarding supernatant HBSS, the pellets were re-suspended in 1 ml HBSS and spun as above. The HBSS remnant was extracted and the cells were put into suspension with serum-free culture medium with supplements (49 ml Neurobasal medium (1x), 1 ml b27 supplement (50x), 10 µl FGF-basic human (100 µg/ml), 10 µl EGF recombinant (mouse) (100 µg/ml), Glutamax 500 µl (200 mM), 500 µl Penicillin/Streptomycin (100x). All reagents were from Invitrogen). The poly-L-ornithine solution was removed and each well was washed with PBS once. Granule neuron precursors were then plated in serum-free culture medium with supplements at a concentration of 2 million cells/well and grown at 37°C and 5% CO2.

Neural forebrain precursor cells

Murine neural forebrain precursors were isolated from the ventricular zone at postnatal day 0 (P0). The mouse cerebrum was separated from the midbrain using a razor blade, in order to achieve a smooth frontal section through the occipital cerebral hemispheres. Basal forebrain structures, the bulbi olfactorii and choroid plexus tissue were removed. Tissue from both cerebral hemispheres was then suspended in 37ºC brain lysis buffer (5

ml Leibovitz´s medium (Pan-Biotech), 250 µl DNAse (Invitrogen), 50 µl Papain (Miltenyi Biotech), 5 µl of 500 mM EDTA). A cell suspension was then prepared by pipetting with a sterile 1000 µl filter tip for 5 minutes. The suspension was incubated at 37ºC in water bath for 20 minutes. The suspended cells were centrifuged at 1000 rpm at room temperature for 5 minutes and re-suspended in 4ml of warm Leibovitz´s medium and centrifuged again for 5 minutes at room temperature. In presence of red blood cells, the washing with Leibovitz´s medium was repeated as described above. Neurosphere culture medium (45.5 ml DMEM-F12 (Pan-Biotech), 2 ml of 1M HEPES buffer (Sigma), 1 ml of b27 growth supplement (Invitrogen), 500 µl of Glutamax (200 mM, Gibco), 500 µl of Non-essential amino acids (100x, Sigma), 500 µl of Pen/Strep (100x, Invitrogen), 20 ng/ml mouse epidermal growth factor (100 µg/ml, Invitrogen), 10 µl FGF-basic human (100 µg/ml)) was then used to bring cells in suspension. Before plating cells in 5 ml dishes the cell suspension was passed through a 70 µm cell strainer, in order to assure a single cell suspension. Cells were grown at 37°C and 5% CO2, cytokines (EGF, FGF) were supplemented every 3 days.

2.5 Colorimetric MTT-assay

The colorimetric MTT (3-(4,5-dimethylthiazol-2-yl)-2,5-diphenyltetrazolium bromide)- assay is a spectrophotometer-based method used to quantify cell growth or cytotoxicity rates (Finlay et al. 1986, Vistica et al. 1991). The tetrazolium salt MTT is chemically reduced by ribosomes in metabolic active cells, forming formazan crystals. The resulting change of solution colour is than quantified through spectrophotometrical absorbance measure. For this work, the Cell Proliferation Kit I (MTT) from Roche was used. Cells were first seeded in 100 µl in 96-well plates at a concentration of $2x10^4$/well and incubated (37ºC) in neurobasal culture medium with supplements (see also primary cell culture) for 16 hours. Spectrophotometrical absorbance was determined using the FLUOstar Optima (BMG labtech) system. For lithium chloride treatment, start point of therapy was defined by adding 10 µl of the MTT reagent to at least three wells and adding the Solubilisation solution (100 µl) after 4 hours, in order to quantify cell viability at time point 0 (T_0). After 24 hours (T_1), 10 µl of the MTT reagent were put into the remaining wells (at least in triplicates) for 4 hours, after which, the Solubilisation solution (100 µl) was added into each well. One well was left without MTT and served as a blank sample. The plates were let sit in the incubator overnight and the optical density (OD) at T_0 and T_1 was de-

termined as follows: $OD_T - OD_{blank}$. Cell viability after 24 hours (T_1) was calculated using the following formula: OD_{T0}/OD_{T1}= 100%/x.

2.6 Lithium chloride treatment

In our *in vitro* setting, lithium chloride was balanced with NaCl in order to achieve equal salt concentrations of 25 mM in every well. Lithium chloride dosage for *in vivo* treatment was chosen according to previous publications (Makoukji et al. 2012). *Math1-cre::SmoM2$^{Fl/+}$* mice underwent daily intraperitoneal injections of either 50 mg/kg lithium chloride (LiCl) or sodium chloride (NaCl) for 10 days starting from P15. LiCl and NaCl were diluted in sterile H_2O.

2.7 Allotransplantation

Forebrain tumor cells from *hGFAP-cre::Ctnnb1(ex3)$^{Fl/+}$SmoM2$^{Fl/+}$* mice at postnatal day 0 (P0) were isolated and put into primary culture for 4 days, as described above. After Xylazine-Ketamine anesthesia (Xylazine: 5mg/kg body weight, Ketamine: 100mg/kg body weight), the skin of *NMRI-Nu/Nu* mice was cut in order to expose the skull and a burr hole craniotomy was performed. A 2 µl suspension containing 400.000 forebrain tumor cells from *hGFAP-cre::Ctnnb1(ex3)$^{Fl/+}$SmoM2$^{Fl/+}$* mice were injected stereotactically into the brain. Counting the intersection between the coronal and sagittal suture (also called Bregma point) as position 0, following coordinates were used: *caudal*: 2.2 mm, *lateral (right)*: 2 mm, *ventral*: 2 mm.
Transplanted mice were monitored for neurological dysfunctions on a daily basis and sacrificed upon occurrence of general or neurological symptoms.

2.8 RNA extraction, cDNA synthesis and RT PCR

Both cultured cells and tissue samples were first put into Eppendorf tubes and homogenised with 750 µl TRIzol® (Invitrogen) reagent using a pipette, before proceeding with RNA extraction. The homogenised samples were let sit at room temperature for about 5 minutes. 150 µl of chloroform were added to each tube. After mixing for 15 seconds, the samples were incubated at room temperature for 3 minutes. A centrifugation step with 14.000 rpm at 4ºC was conducted for 15 minutes, after which the supernatant, RNA-containing top layer was extracted into a new Eppendorf tube. The RNA was then precipitated with cold (4ºC) isopropanol and incubated at room temperature for 10 minutes. A centrifugation step was repeated as described above. Eventually, the RNA pellet be-

came visible at the bottom of the tubes. The supernatant liquid was discarded and the RNA pellet was washed with 75% ethanol. After brief shaking, each sample was centrifuged for 5 minutes at 4ºC with 7500 rpm. Ethanol was discarded, and the RNA pellets were re-suspended in 24 µl DEPC water each. The RNA concentration was determined through Nanodrop 3300 technology (Thermo Fischer Scientific). cDNA Synthesis for RT PCR was performed using SuperScript® III First-Strand Synthesis Supermix (Invitrogen). Each component was mixed and centrifuged before use. For each RNA sample the reaction mix consisted of the following reagents: 6 µl of RNA (in DEPC water, up to 5 µg RNA), 0.5 µl oligo$(dT)_{20}$ primer (50 µM), 0.5 µl of random hexamers (50 ng/µl), 1 µl annealing buffer , RNAse/DNAse-free water to bring the total volume up to 8 µl. After heating at 65ºC for 5 minutes in a thermo-cycler, the tubes were put on ice for 1 minute. Leaving the tubes on ice, the following solutions were added to each reaction mix: 10 µl First-Strand Reaction Mix (2x), 2 µl SuperScript® III/ RNaseOUT™ Enzyme Mix. The tubes were than mixed by vortexing and centrifuged briefly. The samples were incubated in a thermo-cycler for 5 minutes at 25ºC, 50 minutes at 50ºC and finally at 85ºC for 5 minutes. Finally, the cDNA was cooled down on ice and stored at -20ºC.

Reverse Transcriptase PCR (RT PCR)

Reverse Transcriptase PCR (RT PCR) was carried out using the LightCycler® 480 (Roche) technology and the LightCycler® 480 SYBR Green I Master Mix (Roche). SYBR Green is a fluorescent cDNA-intercalating dye, which is detected and quantified after each elongation step, therefore allowing cDNA quantification in real time. Each reaction mix contained the following agents: FastStart Taq DNA Polymerase and SYBR Green dye (Roche), 3 µl of cDNA, 1 µl forward primer and 1 µl reverse primer (primer stocks concentration: 100 pmol/µl). Before usage, each primer was diluted 1:10 in DNAse free water. A RT PCR program was conducted, which included the following steps: heat shock at 95ºC for 5 minutes (once), then 45-cycles containing the following steps: denaturation at 95ºC for 10 seconds, annealing at 57-62ºC for 10 seconds, elongation at 72ºC for 15 seconds.

Relative quantification was achieved by comparing cDNA levels between target genes and housekeeper genes (*β2-Microglobulin* (*β2M*)). Besides this, a calibrating sample was used for each LightCycler® run within a single experiment, in order to compensate variations of the reaction mix composition. All samples were analysed in triplicates. The following formula was applied for relative quantification:

$$NR = E_T^{CpT(C) - CpT(S)} \times E_R^{CpR(S) - CpR(C)}$$

NR= normalized ratio, E= primer efficiency, T= target gene, C= calibrating sample, R= housekeeper gene, S= sample, Cp= crossing point (number of cycles after which the SYBR Green detection threshold is reached).

All primers were designed using the Primer3 software and ordered from Eurofins Genomics. Amplicon melting curves were analysed to determine the presence of a single PCR product, primer quality and primer efficiencies were calculated based on standard curves. **Table 1** shows primer pairs sequences and efficiencies.

Table 1.

gene	sequence	efficiency	annealing
β2M Fw	CCTGGTCTTTCTGGTGCTTG	2.23	60ºC
β2M Rv	TATGTTCGGCTTCCCATTCT		
Axin2 Fw	GCTGGTTGTCACCTACTTTTTCT	1.81	62ºC
Axin2 Rv	ATTCGTCACTCGCCTTCTTG		
Dkk1 Fw	CTGACCACAGCCATTTTCCT	1.88	62ºC
Dkk1 Rv	ACGGAGCCTTCTTGTCCTTT		
Ptch1 Fw	TATCCCTGCCCTGCGAGCGT	1.91	60ºC
Ptch1 Rv	CCTGCTGACACAGGGGCTTGT		
cMyc Fw	CTCAGTGGTCTTTCCCTACCCG	1.869 (Reed et al. 2008)	60ºC
cMyc Rv	TGTCCAACTTGGCCCTCTTGGC		
Tcf7l2 Fw	AGCAGACAAACCCTCAAGGA	1.926	62ºC
Tcf7l2 Rv	TAAGTGCGGAGGTGGATTTC		

2.9 Histology and immunohistochemistry

After dissection, all brains were fixed with 4% paraformaldehyde at 4ºC. For Hematoxylin and Eosin (H.E.) staining, the tissue was dehydrated, embedded in paraffin and sectioned at 5 µm according to established protocols. For immunohistochemistry, 4 µm sections were gained from the paraffin-embedded tissue and rehydrated. Immunohistochemical staining for Ki67 (primary antibody from Abcam, 1:200) was obtained using the

automated iView DAB Detection Kit (Ventana®). Histological imaging was performed using Olympus Bx41 and Bx50 microscopes with the Cell software or the Color view Soft imaging system (Olympus).

2.10 Protein extraction and western blot

Cell pellets or tissues were put into an Eppendorf tube and 50 µl cold (4ºC) Lysis buffer (50 mmol/L Tris-HCl (pH 8), 120 mmol/L NaCl, 0.5% Nonidet P-40, 1 mmol/L phenymetylsulfonyl fluoride (Sigma), 100 U/ml Aprotinin (Calciobiochem), 0.1 mol/L NaF) was added. The tubes were left on ice and stirred on an orbital shaker for 30 minutes. The samples were than centrifuged at 4ºC for 20 minutes with 12,000 G. The protein-containing supernatant was than extracted and put into a new tube. Electrophoresis on 10% sodium dodecylsulfate polyacrylamide gel was performed and blotting was conducted on nitrocellulose membrane. Ponceau staining was used to estimate the loading of each well. 5% non-fat dry milk (BioRad) in PBS-Tween was utilized to block the membranes for 2 hours at room temperature. Primary antibodies were diluted (Beta tubulin 1:500 (Sigma), Gli2 1:500 (Abcam), Axin2 1:200 (Abcam)) in PBST and let incubate at 4ºC overnight. An alkaline phosphatase-labelled goat secondary antibody and the CDP-Star solution (Roche) were used for chemiluminescence detection.

2.11 Statistical analysis

The Prism5 software was used for statistical analysis. Survival data were obtained through Kaplan-Meyer curves and the Log-rank test served as significance test. P- values <0.05 were considered as significant. Survival curves for *Math1-cre::SmoM2*$^{Fl/+}$ mice were drafted having *n*=15 LiCl and *n*=10 NaCl mice. Survival data for allotransplanted NMRI-*Nu/Nu* mice were calculated on *n*=8 animals. When comparing two groups with assumed Gaussian distribution and equal variances, the unpaired t-test was conducted. In case of not equal variances or an expected non-Gaussian distribution, the non-parametric Mann-Whitney test was used. For RT PCR, western blot and MTT-assays a number of at least three samples was analysed for each experimental condition or mouse genotype.

3. Results

3.1 Effects of activated Wnt/ β-Catenin signaling on Shh-dependent medulloblastoma formation

3.1.1 In vitro treatment of granule neuron progenitors and medulloblastoma tumor cells with the Wnt agonist lithium chloride

Lithium is a chemical element with psychotropic properties, which is commonly used to treat bipolar disorder as well as other psychiatric diseases (Geddes et al. 2004, Storosum et al. 2007), although the underpinnings of its biochemical effects remain only partially understood (Alda 2015). Among others, Lithium has been shown to act as an inhibitor of Glycogen synthase kinase 3 beta, a serine/threonine kinase also known as GSK3B (Klein et al. 1996, Stambolic et al. 1996, O'Brien et al. 2009). GSK3B is part of the so-called cytoplasmic destruction complex together with Axin, Adenomatosis polyposis coli (APC), Dishevelled (Dvl), the CK1-Kinase group and GSK3A (Clevers 2006). This protein complex leads to phosphorylation, ubiquitination, and therefore proteasomal degradation of β-Catenin in the cytoplasm. (Aberle et al. 1997, Willert et al. 1999). Hence, Lithium is able to activate the Wnt/ β-Catenin pathway by inhibiting GSK3B and therefore preventing phosphorylation and subsequent degradation of β-Catenin (Stambolic et al. 1996). Previous results demonstrated an inhibitory effect of constitutional Wnt/ β-Catenin activation on Shh-dependent medulloblastoma formation in *Math1-cre::SmoM2*$^{Fl/+}$*::Ctnnb1(ex3)*$^{Fl/+}$ mice (Pöschl et al. 2014). In order to examine, whether a Wnt agonist might represent a suitable treatment option for patients with Shh-dependent medulloblastoma, a series of *in vitro* and *in vivo* experiments was conducted, in order to inquire a possible inhibitory effect of lithium chloride (LiCl), a highly soluble lithium salt, which has been suggested to act as a Wnt/ β-Catenin activator in the cerebellum (Lancaster et al. 2011). First, MTT (3-(4,5-dimethylthiazol-2-yl)-2,5-diphenyltetrazolium bromide) assays were carried out to investigate, whether the treatment of medulloblastoma tumor cells with LiCl would result in a decrease of cell viability *in vitro* **(Figure 8)**. Granule neuron precursor cells (GNPs), from which Shh-dependent medulloblastoma arise (Schüller et al. 2008), as well as medulloblastoma tumor cells from *Math1-cre::SmoM2*$^{Fl/+}$ and *Ptch1*$^{+/-}$ mice, two well-known murine models for Shh-induced medulloblastoma (Goodrich et al. 1997, Schüller et al. 2008), were isolated and put into primary culture for 16 hours. These cells were than treated with 10 mM LiCl for 24 hours in parallel with HEK293T, UW473 and GL261 cell lines (see methods section),

which served as Shh-independent control cells. As a result, LiCl lead to a significant decrease of cell viability in Shh-dependent GNPs and tumor cells from *Math1-cre::SmoM2*$^{Fl/+}$ and *Ptch1*$^{+/-}$ mice when compared to control cells ($p<0.01$) (Pöschl et al. 2014) **(Figure 8)**. Thus, LiCl is able to inhibit proliferation of Shh-associated medulloblastoma cells *in vitro* (Pöschl et al. 2014).

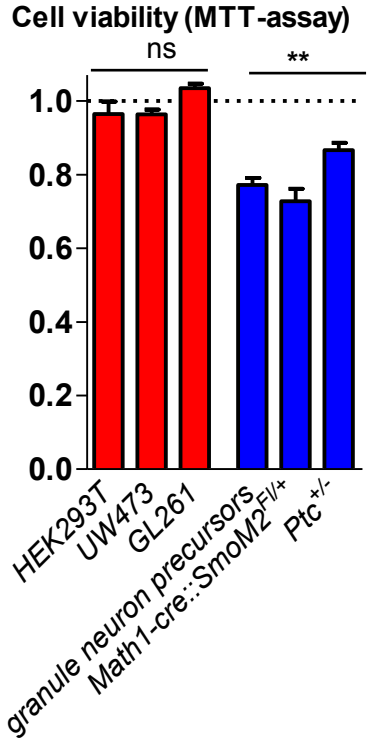

Figure 8. Lithium chloride (LiCl) reduces medulloblastoma cell viability *in vitro.* Colorimetric MTT assays after 24h *in vitro* treatment with 10 mM LiCl decreased cell viability of granule neuron precursor cells and medulloblastoma tumor cells from *Math1-cre::SmoM2*$^{Fl/+}$ and *Ptch1*$^{+/-}$ mice, when compared to HEK293T, UW473 and GL261 control cells (Pöschl et al. 2014). $p<0.01$, one sample t-test. Bars show mean with SEM. *ns* not significant. *Two asterisks* $p<0.01$.

3.1.2 In vivo treatment of medulloblastoma using the Wnt agonist lithium chloride

Following the *in vitro* investigations, *in vivo* experiments on *Math1-cre::SmoM2*$^{Fl/+}$ mice were initiated, in order to examine, whether LiCl might unfold an inhibitory effect on tumor formation in a murine medulloblastoma model. *Math1-cre::SmoM2*$^{Fl/+}$ mice were treated with i.p. injections of 50 mg LiCl (n=15) or NaCl (n=10) per gram body weight/day starting from P15 for 10 days, having their gross motoric functions monitored on a daily basis. A survival analysis was conducted counting the appearance of tumor-related symptoms with subsequent sacrifice as statistical endpoints **(Figure 9A)**. Under this ex-

perimental setup, the LiCl group failed to show a statistically relevant survival benefit when compared to the Nacl-treated control group (p=0.2734). RT-PCR studies on medulloblastoma samples from both LiCl and NaCl-treated *Math1-cre::SmoM2*$^{Fl/+}$ mice (NaCl: *n*=3; LiCl: *n*=3) suggested the inability of LiCl to enhance, under our treatment protocol, the relative expression of *Axin2*, *c-Myc*, *Dkk1* and *Tcf7l2* (also known as *TCF-4*), which are well-known Wnt/ β-Catenin target genes (He et al. 1998, Yan et al. 2001, Niida et al. 2004, Brown et al. 2012) **(Figure 9B)**. Thus, under the examined conditions, LiCl was not able to induce Wnt target genes expression *in vivo,* explaining the lacking effect on overall survival of treated *Math1-cre::SmoM2*$^{Fl/+}$ mice. *In vitro* experiments showed that Wnt agonists can represent a promising treatment option for Shh-dependent medulloblastoma. However, the right substance, dose and application method for *in vivo* treatment still has to be defined.

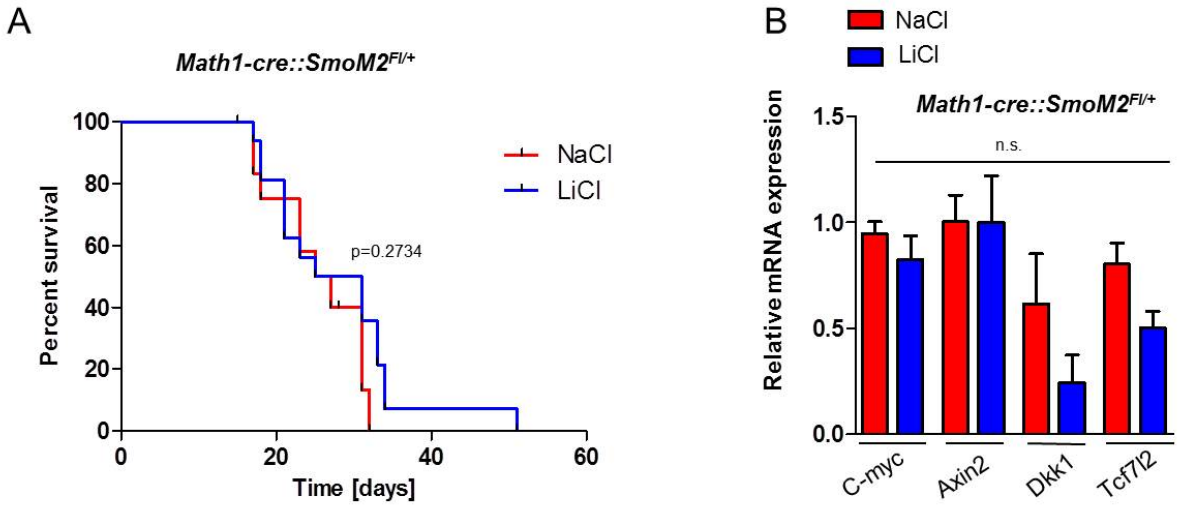

Figure 9. *In vivo* lithium chloride (LiCl) treatment leads to no Wnt activation or survival benefit in *Math1-cre::SmoM2*$^{Fl/+}$ medulloblastoma mice. (A) Kaplan-Meyer curves comparing *Math1-cre::SmoM2*$^{Fl/+}$ mice survival after LiCl or NaCl treatment showed no significant survival benefit of the LiCl-treated mice. (p=0.2734, Log-rank Mantel-Cox test. Censored mice: NaCl n=5, LiCl n=6.). **(B)** *Math1-cre::SmoM2*$^{Fl/+}$ tumor mice were treated daily with 50 mg LiCl (*n*=15) or NaCl (*n*=10) per gram body weight starting from P15 for 10 days. RT PCR studies showed no up-regulation of Wnt-associated target genes in tumor tissue after LiCl (*n*=3) or NaCl (*n*=3) treatment. Target genes were normalized to *β2-Microglobulin* (*β2M*) mRNA. *Bars* show mean with SEM.

3.2 The role of activated Shh and Wnt/ β-Catenin signaling in embryonal tumors with multilayered rosettes (ETMR)

3.2.1 Activation of Shh and Wnt/ β-Catenin in *hGFAP*-positive neural forebrain precursor cells induces embryonal forebrain tumors in mice

Recent studies show, based on global gene expression analysis, an upregulation of

Sonic hedgehog (Shh) and Wnt/ β-Catenin targets in a particular subgroup of primitive neuroectodermal tumors (PNET) of the central nervous system (Picard et al. 2012), which can be identified with the recently coined term of “Embryonal tumor with multi-layered rosettes” (ETMR) (Paulus et al. 2010, Wesseling 2014). With the purpose of investigating the possible effects of Shh and Wnt/ β-Catenin signaling in ETMR tumorigenesis and in order to establish a mouse model for ETMRs, *hGFAP-cre::Ctnnb1(ex3)$^{Fl/+}$SmoM2$^{Fl/+}$* mice were generated (see breeding scheme Figure 5). These transgenic mice are characterized by a constitutional and simultaneous Shh and Wnt/ β-Catenin activation under the control of the *hGFAP* promotor (Zhuo et al. 2001). In order to characterize the brain morphology of these mice, sagittal histological sections at P0 were carried out. While the control *Ctnnb1(ex3)$^{Fl/+}$SmoM2$^{Fl/+}$* mice showed normal development of fore- and hindbrain structures **(Fig 10A)** with proliferating cells in the ventricular zone **(Figure 10E)**, *hGFAP-cre::Ctnnb1(ex3)$^{Fl/+}$SmoM2$^{Fl/+}$* brains revealed the formation of extensive forebrain tumors involving both cerebral hemispheres **(Figure 10D)**, which displayed high mitotic activity, as indicated by ki67 staining **(Figure 10H)**. The formation of tumors was unique in the condition with both pathways being simultaneously active, since (1) *hGFAP-cre::Ctnnb1(ex3)$^{Fl/+}$* mice, a conditional mouse model featuring constitutional Wnt/ β-Catenin activation through β-Catenin mutation **(Figure 10B)**, showed a disruption of the overall brain morphology as already published (Pöschl et al. 2013) and (2) *hGFAP-cre::SmoM2$^{Fl/+}$* mice **(Figure 10C)** displayed a hyperproliferative, thickened ventricular zone, that was not seen at later stages **(Figure 10 inlay, P18)**, but no forebrain tumor formation (*hGFAP-cre::Ctnnb1(ex3)$^{Fl/+}$* and *hGFAP-cre::SmoM2$^{Fl/+}$* samples were provided by Dr. Julia Neumann). *hGFAP-cre::SmoM2$^{Fl/+}$* mice revealed, as expected, medulloblastoma formation in the cerebellum (Grammel et al. 2012). Therefore, it can be concluded that constitutional activation of both Wnt/ β-Catenin and Shh in *hGFAP*-positive cells appears to be required and sufficient to induce forebrain tumors in *hGFAP-cre::Ctnnb1(ex3)$^{Fl/+}$SmoM2$^{Fl/+}$* mice. In contrast, the single activation of either Shh or Wnt/ β-Catenin is not sufficient to generate the same phenotype, as observed in *hGFAP-cre::SmoM2$^{Fl/+}$* or *hGFAP-cre::Ctnnb1(ex3)$^{Fl/+}$* mice. At higher magnification, *hGFAP-cre::Ctnnb1(ex3)$^{Fl/+}$SmoM2$^{Fl/+}$* forebrain tumors were characterized by diffuse, densely packed tumor cells with round or polygonal nuclei **(Figure 10I)**. Similarly to human ETMR samples (Korshunov et al. 2010), histological slides from *hGFAP-cre::Ctnnb1(ex3)$^{Fl/+}$SmoM2$^{Fl/+}$* mice showed areas resembling multi-layered ro-

settes, consisting of a tumor cell halo surrounding a cell-free, acidophilic zone **(Figure 10J,I arrows)**.

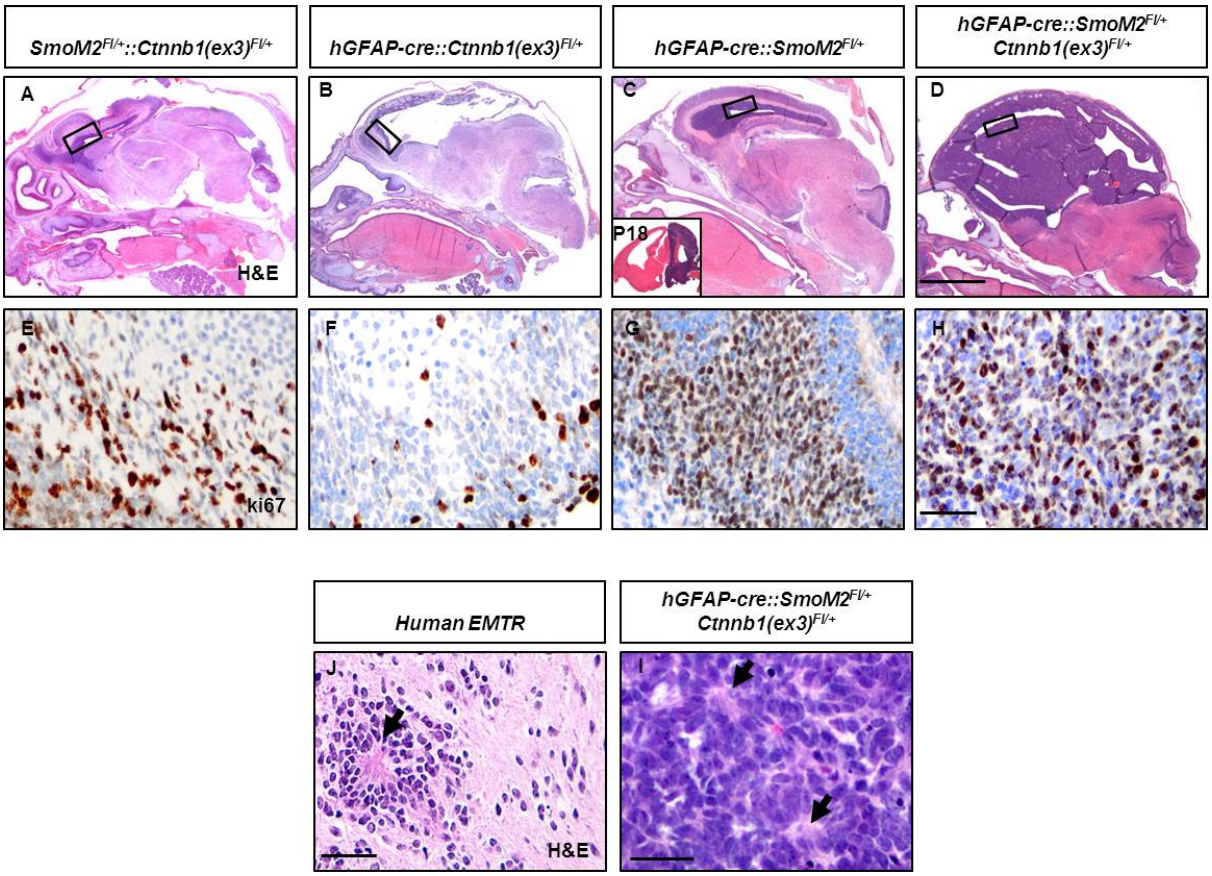

Figure 10. Activation of both Shh and Wnt/ β-Catenin in *hGFAP*-positive neural forebrain precursor cells induces embryonal forebrain tumors in mice. (D) *hGFAP-cre::Ctnnb1(ex3)$^{Fl/+}$ SmoM2$^{Fl/+}$* mice at P0 showed extensive forebrain tumors involving both cerebral hemispheres. **(A-C)** *Ctnnb1(ex3)$^{Fl/+}$ SmoM2$^{Fl/+}$* control mice showed, as expected, no brain abnormalities. *hGFAP-cre::Ctnnb1(ex3)$^{Fl/+}$* mice featured a disruption of the forebrain and cerebellum morphology, as previously described in Pöschl et al. 2013. *hGFAP-cre::SmoM2$^{Fl/+}$* mice presented medulloblastoma formation (Grammel et al. 2012) in the cerebellum and no disruption of the overall forebrain architecture. Nevertheless, *hGFAP-cre::SmoM2$^{Fl/+}$* mice revealed a hyperproliferative, thickened ventricular zone in the forebrain, which was no longer detectable at P18 **(C, inlay)** and lead to no tumor formation (*hGFAP-cre::Ctnnb1(ex3)$^{Fl/+}$*, *hGFAP-cre::SmoM2$^{Fl/+}$* and *hGFAP-cre::Ctnnb1(ex3)$^{Fl/+}$ SmoM2$^{Fl/+}$* samples were provided by Julia Neumann). **(E-H)** Ki67 stainings indicated the presence of diffuse, highly proliferative cells within *hGFAP-cre::Ctnnb1(ex3)$^{Fl/+}$ SmoM2$^{Fl/+}$* forebrain tumors when compared to control genotypes. **(J-I)** *hGFAP-cre::Ctnnb1(ex3)$^{Fl/+}$ SmoM2$^{Fl/+}$* forebrain tumors appeared to resemble some histological features of human ETMRs, such as the formation of multilayered rosettes **(arrows)**. *H&E* Hematoxylin and eosin stain. (A,D) sagittal sections. Scale bar in D is 1 mm for A,B,C,D. Scale bar in H is 50 µm for E,F,G,H. Scale bar in J is 50 µm. Scale bar in I is 50 µm.

3.2.2 Activation of Shh and Wnt/ β-Catenin in *hGFAP*-positive neural forebrain precursor cells leads to increased proliferation *in vitro*

Having discovered that constitutional and simultaneous Shh and Wnt/ β-Catenin activa-

tion is able to induce tumor formation in the forebrain of *hGFAP-cre::Ctnnb1(ex3)$^{Fl/+}$SmoM2$^{Fl/+}$* mice, *in vitro* experiments were carried out, aiming at a morphological and molecular characterization of the induced tumor cells. Neural forebrain precursor cells were isolated from the ventricular zone of *hGFAP-cre::Ctnnb1(ex3)$^{Fl/+}$SmoM2$^{Fl/+}$* mice at P0 and put into primary cell culture for 4 days (see methods section). The cultured cells appeared to form cell clusters or spheres **(Figure 11A)**, whose diameter and density were significantly higher than in the wild type condition (p=0.0007, p<0.0001 respectively) **(Figure 11B and C)**.

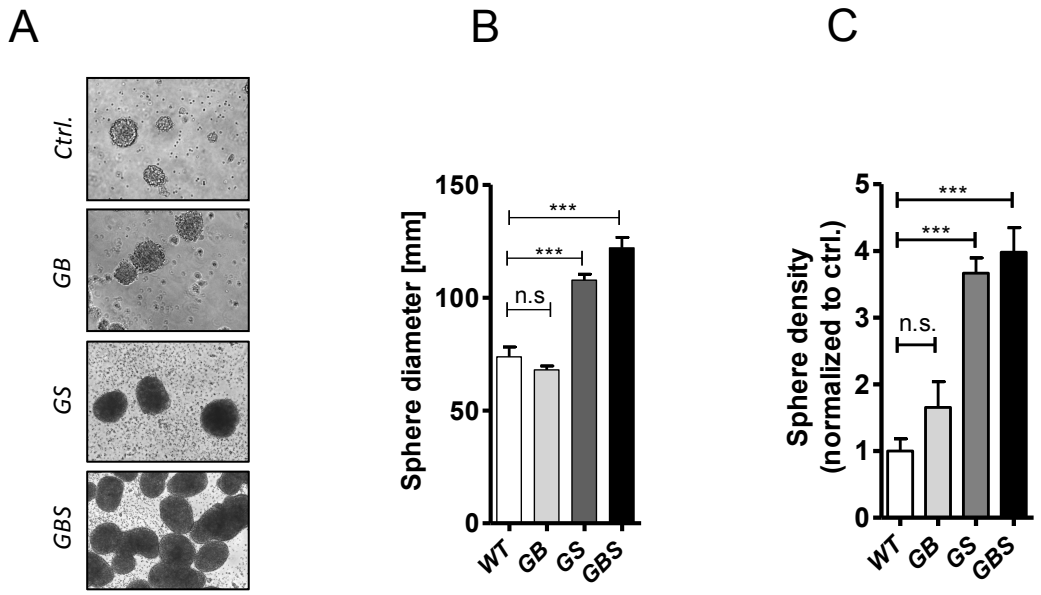

Figure 11. Activation of both Shh and Wnt/ β-Catenin in *hGFAP*-positive neural forebrain precursor cells from *hGFAP-cre::Ctnnb1(ex3)$^{Fl/+}$SmoM2$^{Fl/+}$* mice leads to increased proliferation *in vitro*. (A) Neural forebrain precursor cells from the ventricular zone of *hGFAP-cre::Ctnnb1(ex3)$^{Fl/+}$SmoM2$^{Fl/+}$* mice were isolated at P0 and placed into primary culture for 4 days, leading to the formation of densely packed cell spheres. Neural forebrain precursor cells from wild type, *hGFAP-cre::Ctnnb1(ex3)$^{Fl/+}$* and *hGFAP-cre::SmoM2$^{Fl/+}$* mice were cultured following the same protocol (see methods section). **(B,C)** *hGFAP-cre::Ctnnb1(ex3)$^{Fl/+}$SmoM2$^{Fl/+}$* spheres showed an increased diameter and density when compared to wild type cells (p=0.0007 and p=<0,0001 respectively, unpaired t-test). Similar findings were observed for *GFAP-cre::SmoM2$^{Fl/+}$* spheres (diameter p= 0.0005; density p= <0.0001, unpaired t-test). This was consistent with the hyperproliferative ventricular zone detected in *hGFAP-cre::SmoM2$^{Fl/+}$* forebrains at P0 (see Figure 10). *Bars* show mean with SEM. *ns* not significant. GB *hGFAP-cre::Ctnnb1(ex3)$^{Fl/+}$*. GS *GFAP-cre::SmoM2$^{Fl/+}$*. GBS *hGFAP-cre::Ctnnb1(ex3)$^{Fl/+}$SmoM2$^{Fl/+}$*, *WT* Wild-type. *Three asterisks* p<0.001.

hGFAP-cre::Ctnnb1(ex3)$^{Fl/+}$ spheres were not increased in comparison to control spheres, whereas *hGFAP-cre::SmoM2$^{Fl/+}$* spheres revealed an increased diameter (p=0.0005) and density (p<0.0001). These results were consistent with the previously described detection of a hyperproliferative ventricular zone in *hGFAP-cre::SmoM2$^{Fl/+}$*

forebrains at P0. Hence, the *hGFAP*-positive neural forebrain precursor cell population originating from *hGFAP-cre::Ctnnb1(ex3)*$^{Fl/+}$*SmoM2*$^{Fl/+}$ mice presents an increased proliferation rate when compared to control genotypes.

3.2.3 Interplay of Shh and Wnt/ β-Catenin signaling pathways in murine embryonal forebrain tumors *in vitro* and *in vivo*

In order to characterize Shh and Wnt/ β-Catenin signaling in the above mentioned spheres, RT-PCR studies were conducted to determine the mRNA expression patterns of *Patched-1 (Ptch1),* a well-known Shh target gene, and *Axin2*, a well-known Wnt/ β-Catenin target gene (Yan et al. 2001, Robbins et al. 2012) **(Figure 12)**.

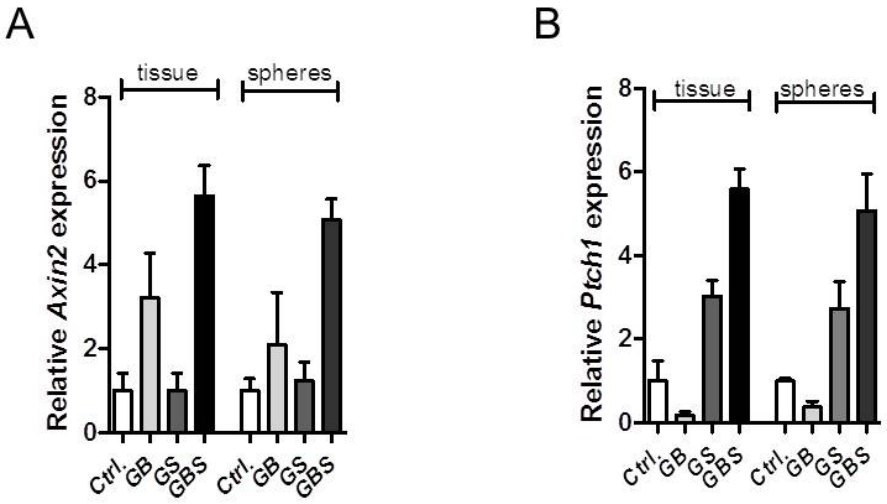

Figure 12. Synergistic effects of Shh and Wnt/ β-Catenin in murine embryonal forebrain tumors *in vivo* and *in vitro*. (A,B) Real time PCR studies on *hGFAP-cre::Ctnnb1(ex3)*$^{Fl/+}$ *SmoM2*$^{Fl/+}$ mRNA from both forebrain tumor tissue and neural forebrain precursor spheres demonstrated a relative overexpression of *Axin2 and Patched-1 (Ptch1)*; respectively, two well-known Wnt/ β-Catenin and Shh target genes. The relative expression of both *Axin2* and *Ptch1* in *hGFAP-cre::Ctnnb1(ex3)*$^{Fl/+}$ *SmoM2*$^{Fl/+}$ tissue and cell spheres appeared to be more elevated than in the *hGFAP-cre::Ctnnb1(ex3)*$^{Fl/+}$ or *GFAP-cre::SmoM2*$^{Fl/+}$ conditions, thus suggesting a possible synergistic effect of Shh and Wnt/ β-Catenin signalling in *hGFAP-positive* cells of the forebrain, perhaps in terms of a reciprocal pathway activation. Target genes were normalized to *β2-Microglobulin* (*β2M*) mRNA. GB *hGFAP-cre::Ctnnb1(ex3)*$^{Fl/+}$. GS *hGFAP-cre::SmoM2*$^{Fl/+}$. GBS *hGFAP-cre::Ctnnb1(ex3)*$^{Fl/+}$ *SmoM2*$^{Fl/+}$. *Bars* show mean with SEM.

As expected, the relative expression of *Axin2* and *Ptch1* was enhanced in *hGFAP-cre::Ctnnb1(ex3)*$^{Fl/+}$*SmoM2*$^{Fl/+}$ forebrain tumor samples as well as in cultured neural forebrain precursor spheres **(Figure 12A,B)**, therefore validating our *in vivo* and *in vitro* models. *hGFAP-cre::SmoM2*$^{Fl/+}$ mice showed an increased relative expression of *Ptch1* alone. Similarly, *hGFAP-cre::Ctnnb1(ex3)*$^{Fl/+}$ mice presented sole Wnt/ β-Catenin activation, which was indicated by *Axin2* overexpression. The relative mRNA expression of

both *Ptch1* and *Axin2* in *hGFAP-cre::Ctnnb1(ex3)$^{Fl/+}$SmoM2$^{Fl/+}$* mice showed the tendency to be more elevated when compared to the *hGFAP-cre::SmoM2$^{Fl/+}$* or *hGFAP-cre::Ctnnb1(ex3)$^{Fl/+}$* genotypes, respectively. Hence, the simultaneous activation of Shh and Wnt/ β-Catenin in the forebrain of *hGFAP-cre::Ctnnb1(ex3)$^{Fl/+}$SmoM2$^{Fl/+}$* mice might cause a mutual and synergistic effect of these signalling pathways on each other. In order to verify, whether the mRNA upregulation of Shh and Wnt/ β-Catenin target genes in our mouse model might be confirmed on a post-translational level, a western blot analysis was carried out. Relative protein levels of Axin2 and Gli2, a Shh target gene (Robbins et al. 2012) were quantified by normalization to Beta tubulin expression **(Figure 13 A,B)**. The relative protein expression of both Axin2 and Gli2 in forebrain tumor samples from *hGFAP-cre::Ctnnb1(ex3)$^{Fl/+}$SmoM2$^{Fl/+}$* mice was significantly elevated when compared to *hGFAP-cre* control mice (p=0.0007 and p=0.0333, respectively).

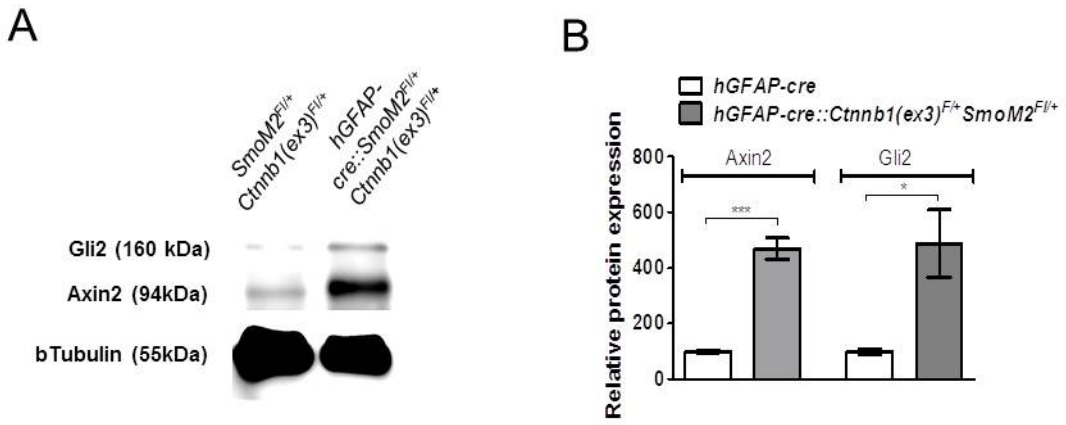

Figure 13. *hGFAP-cre::Ctnnb1(ex3)$^{Fl/+}$SmoM2$^{Fl/+}$* mice show posttranslational overexpression of Shh and Wnt/ β-Catenin targets. The up-regulation of both Shh and Wnt/ β-Catenin signalling pathways in forebrain tumor samples from *hGFAP-cre::Ctnnb1(ex3)$^{Fl/+}$SmoM2$^{Fl/+}$* mice was confirmed through western blot analysis, which showed an increase in relative protein expression of Gli2 (p=0.0333) and Axin2 (p=0.0007) when compared to *hGFAP-cre* control tissue. Target proteins were normalized to Beta Tubulin protein expression. GB *hGFAP-cre::Ctnnb1(ex3)$^{Fl/+}$*. GS *hGFAP-cre::SmoM2$^{Fl/+}$*. GBS *hGFAP-cre::Ctnnb1(ex3)$^{Fl/+}$SmoM2$^{Fl/+}$*. *Bars* show mean with SEM. *Three asterisks* p<0.001. *One asterisk* p<0.05.

3.3 Propagation of Shh and Wnt/ β-Catenin - dependent embryonal forebrain tumors

hGFAP-cre::Ctnnb1(ex3)$^{Fl/+}$SmoM2$^{Fl/+}$ mice succumbed at P0 due to extensive tumoral masses of the cerebral hemispheres, thus making this first EMTR mouse model unsuitable for investigations at later time points. With the objective of creating a viable mouse model for ETMRs and examining the tumor-propagating potential of *hGFAP-*

cre::Ctnnb1(ex3)$^{Fl/+}$*SmoM2*$^{Fl/+}$ tumor cells, neural forebrain precursors were first isolated, put into primary culture and then transplanted into immunodeficient NMRI-*Nu/Nu* (*n*=8) mice **(Figure 14)**. Hematoxylin and eosin staining revealed tumor formation in the host **(Figure 14A, arrows)**, thus demonstrating the ability of *hGFAP-cre::Ctnnb1(ex3)*$^{Fl/+}$*SmoM2*$^{Fl/+}$ forebrain neural precursor cells to propagate after allotransplantation. Allotransplanted tumors showed the histology of densely packed, blue and round cells resembling their primary counterparts and displayed high mitotic activity **(Figure 14B)**. Allotransplanted mice (*n*=8) showed a median survival of 83 days **(Figure 14C)**. Hence, *hGFAP-cre::Ctnnb1(ex3)*$^{Fl/+}$*SmoM2*$^{Fl/+}$ tumor cells can be propagated in host mice, showing that allotransplanted *hGFAP-cre::Ctnnb1(ex3)*$^{Fl/+}$*SmoM2*$^{Fl/+}$ tumor cells can represent a valuable mouse model for ETMRs. This mouse model can be used to further study the biology of ETMRs and perform treatment studies.

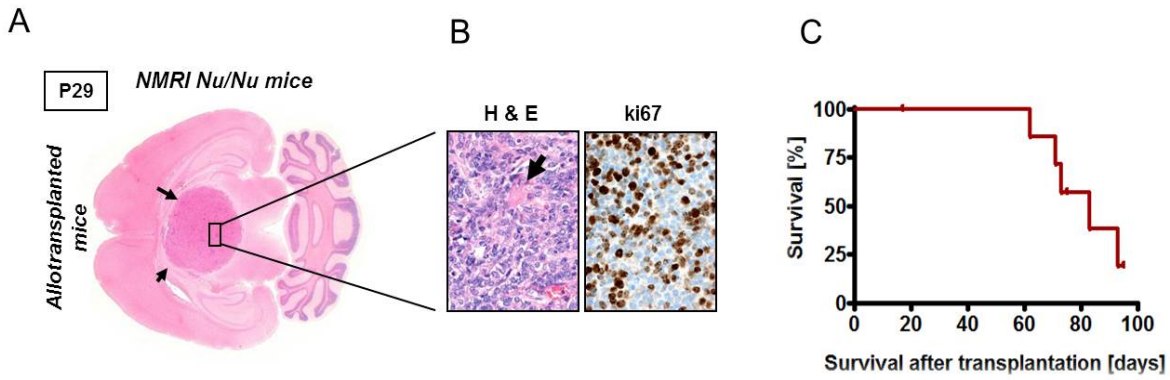

Figure 14. Forebrain tumors of *hGFAP-cre::Ctnnb1(ex3)*$^{Fl/+}$*SmoM2*$^{Fl/+}$ mice are able to propagate after allotransplantation into immunodeficient (*NMRI Nu/Nu)* mice. (A,B) Immunodeficient *NMRI Nu/Nu (n*=8*)* mice underwent stereotactical injection of cultured *hGFAP-cre::Ctnnb1(ex3)*$^{Fl/+}$*SmoM2*$^{Fl/+}$ neural forebrain precursor cells. H.E. and ki67 stainings revealed the formation of secondary tumors, showing densely packed and highly proliferative tumor cells. **(B, arrow)** The affinity with primary *hGFAP-cre::Ctnnb1(ex3)*$^{Fl/+}$*SmoM2*$^{Fl/+}$ forebrain tumors was suggested by the histological evidence of rosettes within the transplanted tumors. **(C)** Allotransplanted mice (*n=8*) showed a reduced median survival of 83 days (censored mice n=3). *H&E* Hematoxylin and eosin stain. (A) Horizontal section.

4. Discussion

Previous studies showed that Wnt/ β-Catenin activation is able to inhibit the Shh-driven proliferation of cerebellar granule neuron precursor cells (CGNPs) (Lorenz et al. 2011) as well as tumor growth in Shh-dependent medulloblastoma (Pöschl et al. 2014). With the intent of investigating, whether the newly discovered inhibitory effect of Wnt over Shh might represent a novel approach in the therapy of Shh-associated medulloblasto-

ma, *in vitro* and *in vivo* experiments on medulloblastoma cells and *Math1-cre::SmoM2*$^{Fl/+}$ mice were conducted using Lithium, a well-known Wnt activator (Stambolic et al. 1996, Lancaster et al. 2011). Results showed that Lithium is able to reduce cell viability of CGNPs and medulloblastoma tumor cells from *Math1-cre::SmoM2*$^{Fl/+}$ and *Ptch1*$^{+/-}$ mice *in vitro* **(Figure 8)** (Pöschl et al. 2014). On the other hand, the *in vivo* treatment of *Math1-cre::SmoM2*$^{Fl/+}$ mice with Lithium under the mentioned experimental setting did not lead to the expected survival benefit. Nevertheless, the relative mRNA expression of Wnt pathway targets genes in medulloblastoma samples from *Math1-cre::SmoM2*$^{Fl/+}$ mice was not elevated after Lithium treatment **(Figure 9)**, thus suggesting that the missing effect on survival might be due to lacking Wnt/ β-Catenin activation. Therefore, considering the encouraging *in vitro* results, it is possible to propose the hypothesis that Wnt activators may represent a valuable therapeutic option for Shh-associated medulloblastoma. Further investigations adopting different dosages of Lithium and other Wnt-activating substances appear therefore to be required. Another type of embryonal tumor of the CNS, the Embryonal tumor with multi-layered rosettes (ETMR), has been recently defined as CNS-PNET subset (Korshunov et al. 2012, Wesseling 2014). Amplification of the chromosome 19q13.41 miRNA polycistron (C19mC) and/or increased *LIN28* expression have been suggested as possible molecular markers for this type of tumor (Korshunov et al. 2014) and are gaining clinical relevance. Furthermore, array-based data from CNS-PNETs revealed a possible overexpression of both Wnt and Shh target genes in a particular subgroup of tumors, which can be identified with the ETMR subset (Picard et al. 2012). With the purpose of examining, whether simultaneous Wnt and Shh activation might induce tumorigenesis in the forebrain, *hGFAP-cre::Ctnnb1(ex3)*$^{Fl/+}$*SmoM2*$^{Fl/+}$ were generated, a conditional mouse model presenting synchronistic Wnt and Shh upregulation in the *hGFAP*-positive cell population. *hGFAP cre::Ctnnb1(ex3)*$^{Fl/+}$*SmoM2*$^{Fl/+}$ mice developed highly proliferative, extensive forebrain tumors with histological resemblance to human ETMRs **(Figure 10)**. RT-PCR and western blot studies confirmed a specular upregulation of the Wnt and the Shh pathway in both tissue samples and cultured forebrain precursor cells from *hGFAP-cre::Ctnnb1(ex3)*$^{Fl/+}$*SmoM2*$^{Fl/+}$ mice, therefore validating our *in vivo* and *in vitro* setting **(Figure 12-13)**. In conclusion, this work was able to establish a mouse model for ETMRs. Furthermore, a viable allotransplantation-based mouse model as well as a cell culture method for ETMR tumor cells have been developed, which might be used for future research. With regard to ETMR pathogenesis, this work was able to show that

constitutional Wnt and Shh activation in the forebrain might lead to ETMR formation *in vivo* as well as increased proliferation of neural forebrain precursor cells *in vitro.* It is therefore legitimate to postulate that Shh and Wnt upregulation might represent a key step in the process of ETMR tumorigenesis. In particular, a possible causal relationship between Shh/ Wnt upregulation and other molecular features of ETMRs, such *LIN28* overexpression or C19mC amplification, should be a matter of further investigation. Furthermore, the newly established mouse model might be helpful in defining the exact cellular origin of EMTRs, which still remains unclear. As far as the interplay between Wnt and Shh is concerned, the results of this work suggest that the interaction between simultaneously activated Wnt and Shh in the CNS might be defined in a spatially-related manner. In fact, simultaneous Wnt and Shh activation appears to unfold diverging effects when comparing forebrain and cerebellum. While Wnt exerts an inhibitory effect over Shh-dependent medulloblastoma in the cerebellum (Lorenz et al. 2011, Pöschl et al. 2014), synchronistic Wnt and Shh activation in the forebrain might be able to induce ETMR formation **(Figure 10-12)**. Moreover, the expression patterns of Wnt and Shh target genes in *hGFAP-cre::Ctnnb1(ex3)*$^{Fl/+}$*SmoM2*$^{Fl/+}$ mice may have revealed a reciprocal, activating interaction between the Wnt and Shh pathway taking place in the forebrain **(Figure 12)**. The molecular mechanisms involved in the interplay between Wnt/ β-Catenin and Shh remain widely unknown, although Gli3-R, the repressive form of the Shh-associated transcription factor Gli3, has been suggested to be play an important role in the modulation of the Wnt/ Shh interplay (Alvarez-Medina et al. 2008). Deeper understanding of the molecular underpinnings characterizing the interaction between these two pathways might shed light onto possible new targets of therapy for embryonal brain tumors, whereas a diverging approach appears to be necessary when considering Shh-dependent medulloblastoma or ETMRs. Indeed, Wnt/ β-Catenin activating substances, such as Lithium (Lancaster et al. 2011), might represent a valuable therapeutic approach for Shh-associated medulloblastoma. ETMR therapy, on contrary, might be focused on molecules curbing the overexpression of both the Wnt and Shh pathway, such as Vismodegib or PKF115-584 (Lepourcelet et al. 2004, Sekulic et al. 2012).

5. Summary

This work investigates the expression and interaction of Shh or Wnt/ β-Catenin in murine Shh-dependent medulloblastoma and ETMRs. The first part of the results focuses on

Shh-dependent medulloblastoma. Previous studies were able to show that Wnt/ β-Catenin activation might be able to inhibit Shh-associated medulloblastoma growth through downregulation of the Shh pathway. Considering a possible therapeutic approach, *in vitro* and *in vivo* treatments with lithium chloride, a well-known Wnt/ β-Catenin agonist, were carried out. Whereas lithium chloride treatment *in vitro* resulted in a decrease of granule neuron precursor and tumor cell viability, *in vivo* treatment of *Math1-cre::SmoM2*$^{Fl/+}$ mice did not show an increased expression of Wnt signalling target genes or a survival benefit under the applied dosage and treatment period. The second part of the results deals with the establishment and characterisation of a mouse model for ETMRs, for which an upregulation of both Wnt/ β-Catenin and Sonic-hedgehog has been recently postulated. In order to achieve a synchronistic activation of these pathways in forebrain precursor cells, *hGFAPcre::Ctnnb1(ex3)*$^{Fl/+}$*SmoM2*$^{Fl/+}$ mice were generated. These mice developed highly proliferative embryonal forebrain tumors, which histologically resembled human ETMRs. RT-PCR and Western blot studies were conducted on both tissue samples and cultured cells from the *hGFAP-cre::Ctnnb1(ex3)*$^{Fl/+}$*SmoM2*$^{Fl/+}$ forebrain tumors, demonstrating an overexpression of both Sonic-hedgehog and Wnt/βCatenin associated targets. Finally, forebrain tumors from *hGFAPcre::Ctnnb1(ex3)*$^{Fl/+}$*SmoM2*$^{Fl/+}$ mice could be propagated into *Nu/Nu* mice. Overall, the results of this work show that the interplay of the Sonic hedgehog and Wnt/ β-Catenin signalling pathway are highly cell- and context specific. The tumor antagonistic effect of Wnt/ β-Catenin signalling on Shh-dependent medulloblastoma growth implicates that Wnt/ β-Catenin agonists could represent a new treatment strategy for these tumors. In forebrain precursor cells, the co-activation of both the Sonic hedgehog and Wnt/ β-Catenin signalling pathway appears to be necessary to induce embryonal tumors, which can be identified as ETMRs. Hence, a detailed understanding of the molecular interplay of these pathways will be needed to further improve targeted therapy. In this context, Wnt or Shh antagonists might be potential candidate drugs for the specific treatment of ETMRs.

6. Zusammenfassung

Diese wissenschaftliche Arbeit untersucht die Expression und Interaktion von Sonic hedgehog (Shh) und Wnt/ β-Catenin in Shh-assoziiertem Medulloblastom und ETMRs durch den Einsatz von Mausmodellen. Der erste Teil der Ergebnisse ist auf das Shh-

induzierte Medulloblastom fokussiert. Vorherige Studien konnten zeigen, dass die Aktivierung von Wnt/ β-Catenin in der Lage ist, das Tumorwachstum von Shh-assoziierten Medulloblastomen durch Shh-Inhibition zu drosseln. Lithium, ein bekannter Wnt Aktivator, wurde in Hinsicht auf einen möglichen therapeutischen Einsatz für eine Reihe von *in vivo*- und *in vitro* Experimenten verwendet. Während Lithium die *in vitro* Proliferation von zerebellären Körnervorläuferzellen und Tumorzellen reduzieren konnte, ergab die *in vivo* Behandlung von *Math1-cre::SmoM2*$^{Fl/+}$ Mäusen keine Überexpression der Wnt-Zielgene sowie keinen Überlebensvorteil unter der applizierten Dosis und dem angewandten Zeitraum. Der zweite Teil der Ergebnisse beschäftigt sich mit der Etablierung und Charakterisierung von einem Mausmodell für ETMRs, für die eine Überexpression von Wnt und Shh neulich nahegelegt wurde. *hGFAPcre::Ctnnb1(ex3)*$^{Fl/+}$*SmoM2*$^{Fl/+}$ Mäuse wurden mit dem Ziel einer synchronistischen Aktivierung dieser Signalwege in Vorderhinrvorläuferzellen generiert. Diese Mäuse zeigten massive, hoch proliferative Tumore des Vorderhirns, die in ihrer Histologie den humanen ETMRs ähnelten. RT PCR und Western blot Analysen demonstrierten eine Überexpression von Shh- und Wnt-assoziierten Zielgenen sowohl im Tumorgewebe als auch in kultivierten Tumorzellen von *hGFAPcre::Ctnnb1(ex3)*$^{Fl/+}$*SmoM2*$^{Fl/+}$ Mäusen. Zudem zeigten die Vorderhirntumore von *hGFAPcre::Ctnnb1(ex3)*$^{Fl/+}$*SmoM2*$^{Fl/+}$ Mäusen die Fähigkeit, in *Nu/Nu* zu propagieren. Zusammenfassend weisen die Ergebnisse dieser Arbeit darauf hin, dass die Interaktion zwischen den Shh und Wnt Signalwegen stark zell- und kontextspezifisch ist. Der inhibitorische Effekt von Wnt/ β-Catenin auf das Shh-abhängige Medulloblastom könnte die Grundlage eines neuen therapeutischen Ansatzes für Medulloblastome sein, bei dem Wnt-aktivierende Substanzen möglicherweise zum Einsatz kommen könnten. Die gleichzeitige Aktivierung von Shh und Wnt scheint zudem nötig zu sein, um Vorderhirntumore zu induzieren, die als ETMRs identifiziert werden können. Dementsprechend wird ein detaillierter Aufschluss der molekularen Interaktion zwischen Shh und Wnt in der Zukunft notwendig sein, um zielgerichtete Therapien entwickeln zu können. Wnt- und Shh-inhibierende Substanzen könnten in diesem Kontext potentielle, spezifische Medikamente für die Therapie von ETMRs darstellen.

6. References

Aberle, H., A. Bauer, J. Stappert, A. Kispert and R. Kemler (1997). "beta-catenin is a target for the ubiquitin-proteasome pathway." EMBO Journal **16**(13): 3797-3804.

Alda, M. (2015). "Lithium in the treatment of bipolar disorder: pharmacology and pharmacogenetics." Molecular Psychiatry **20**(6): 661-670.

Alston, R. D., R. Newton, A. Kelsey, M. J. Newbould, J. M. Birch, B. Lawson and R. J. McNally (2003). "Childhood medulloblastoma in northwest England 1954 to 1997: incidence and survival." Developmental Medicine and Child Neurology **45**(5): 308-314.

Alvarez-Medina, R., J. Cayuso, T. Okubo, S. Takada and E. Marti (2008). "Wnt canonical pathway restricts graded Shh/Gli patterning activity through the regulation of Gli3 expression." Development **135**(2): 237-247.

Athar, M., C. Li, A. L. Kim, V. S. Spiegelman and D. R. Bickers (2014). "Sonic hedgehog signaling in Basal cell nevus syndrome." Cancer Research **74**(18): 4967-4975.

Avaron, F., L. Hoffman, D. Guay and M. A. Akimenko (2006). "Characterization of two new zebrafish members of the hedgehog family: atypical expression of a zebrafish indian hedgehog gene in skeletal elements of both endochondral and dermal origins." Developmental Dynamics **235**(2): 478-489.

Backman, M., O. Machon, L. Mygland, C. J. van den Bout, W. Zhong, M. M. Taketo and S. Krauss (2005). "Effects of canonical Wnt signaling on dorso-ventral specification of the mouse telencephalon." Developmental Biology **279**(1): 155-168.

Bai, C. B., D. Stephen and A. L. Joyner (2004). "All mouse ventral spinal cord patterning by hedgehog is Gli dependent and involves an activator function of Gli3." Developmental Cell **6**(1): 103-115.

Barrow, J. R., K. R. Thomas, O. Boussadia-Zahui, R. Moore, R. Kemler, M. R. Capecchi and A. P. McMahon (2003). "Ectodermal Wnt3/beta-catenin signaling is required for the establishment and maintenance of the apical ectodermal ridge." Genes and Development **17**(3): 394-409.

Barth, A. I., A. L. Pollack, Y. Altschuler, K. E. Mostov and W. J. Nelson (1997). "NH2-terminal deletion of beta-catenin results in stable colocalization of mutant beta-catenin with adenomatous polyposis coli protein and altered MDCK cell adhesion." Journal of Cell Biology **136**(3): 693-706.

Behrens, J., J. P. von Kries, M. Kuhl, L. Bruhn, D. Wedlich, R. Grosschedl and W. Birchmeier (1996). "Functional interaction of [beta]-catenin with the transcription factor LEF-1." Nature **382**(6592): 638-642.

Bobola, M. S., J. R. Silber, R. G. Ellenbogen, J. R. Geyer, A. Blank and R. D. Goff (2005). "O6-Methylguanine-DNA Methyltransferase, O6-Benzylguanine, and Resistance to Clinical Alkylators in Pediatric Primary Brain Tumor Cell Lines." Clinical Cancer Research **11**(7): 2747-2755.

Brown, A. L., D. G. Salerno, T. Sadras, G. A. Engler, C. H. Kok, C. R. Wilkinson, S. E. Samaraweera, T. J. Sadlon, M. Perugini, I. D. Lewis, T. J. Gonda and R. J. D'Andrea (2012). "The GM-CSF receptor utilizes beta-catenin and Tcf4 to specify macrophage lineage differentiation." Differentiation **83**(1): 47-59.

Bumcrot, D. A., R. Takada and A. P. McMahon (1995). "Proteolytic processing yields two secreted forms of sonic hedgehog." Molecular and Cellular Biology **15**(4): 2294-2303.

Castro-Gamero, A. M., K. S. Borges, R. C. Lira, A. F. Andrade, P. F. Fedatto, G. A. Cruzeiro, R. B. Silva, A. M. Fontes, E. T. Valera, M. Bobola, C. A. Scrideli and L. G. Tone (2013). "Chromosomal heterogeneity and instability characterize pediatric medulloblastoma cell lines and affect neoplastic phenotype." Cytotechnology **65**(5): 871-885.

Chenn, A. and C. A. Walsh (2002). "Regulation of cerebral cortical size by control of cell cycle exit in neural precursors." Science **297**(5580): 365-369.

Clevers, H. (2006). "Wnt/β-Catenin Signaling in Development and Disease." Cell **127**(3): 469-480.

Clevers, H. and R. Nusse (2012). "Wnt/beta-catenin signaling and disease." Cell **149**(6): 1192-1205.

Eberhart, C. G. (2011). "Molecular diagnostics in embryonal brain tumors." Brain Pathology **21**(1): 96-104.

Finlay, G. J., W. R. Wilson and B. C. Baguley (1986). "Comparison of in vitro activity of cytotoxic drugs towards human carcinoma and leukaemia cell lines." European Journal of Cancer and Clinical Oncology **22**(6): 655-662.

Freese, J. L., D. Pino and S. J. Pleasure (2010). "Wnt signaling in development and disease." Neurobiology of Disease **38**(2): 148-153.

Gajjar, A., M. Chintagumpala, D. Ashley, S. Kellie, L. E. Kun, T. E. Merchant, S. Woo, G. Wheeler, V. Ahern, M. J. Krasin, M. Fouladi, A. Broniscer, R. Krance, G. A. Hale, C. F. Stewart, R. Dauser, R. A. Sanford, C. Fuller, C. Lau, J. M. Boyett, D. Wallace and R. J. Gilbertson (2006). "Risk-adapted craniospinal radiotherapy followed by high-dose chemotherapy and stem-cell rescue in children with newly diagnosed medulloblastoma (St Jude Medulloblastoma-96): long-term results from a prospective, multicentre trial." Lancet Oncology **7**(10): 813-820.

Geddes, J. R., S. Burgess, K. Hawton, K. Jamison and G. M. Goodwin (2004). "Long-term lithium therapy for bipolar disorder: systematic review and meta-analysis of randomized controlled trials." American Journal of Psychiatry **161**(2): 217-222.

Gibson, P., Y. Tong, G. Robinson, M. C. Thompson, D. S. Currle, C. Eden, T. A. Kranenburg, T. Hogg, H. Poppleton, J. Martin, D. Finkelstein, S. Pounds, A. Weiss, Z. Patay, M. Scoggins, R. Ogg, Y. Pei, Z. J. Yang, S. Brun, Y. Lee, F. Zindy, J. C. Lindsey, M. M. Taketo, F. A. Boop, R. A. Sanford, A. Gajjar, S. C. Clifford, M. F. Roussel, P. J. McKinnon, D. H. Gutmann, D. W. Ellison, R. Wechsler-Reya and R. J. Gilbertson (2010). "Subtypes of medulloblastoma have distinct developmental origins." Nature **468**(7327): 1095-1099.

Giordana, M. T., P. Schiffer, M. Lanotte, P. Girardi and A. Chio (1999). "Epidemiology of adult medulloblastoma." International Journal of Cancer **80**(5): 689-692.

Gjerris, F., N. Agerlin, S. E. Børgesen, L. Buhl, J. Haase, L. Klinken, A. C. Mortensen, J. H. Olsen, N. Ovesen, E. Reske-Nielsen and K. Schmidt (1998). "Epidemiology and prognosis in children treated for intracranial tumours in Denmark 1960–1984." Child's Nervous System **14**(7): 302-311.

Goodrich, L. V., L. Milenkovic, K. M. Higgins and M. P. Scott (1997). "Altered neural cell fates and medulloblastoma in mouse patched mutants." Science **277**(5329): 1109-1113.

Graham, F. L., J. Smiley, W. C. Russell and R. Nairn (1977). "Characteristics of a human cell line transformed by DNA from human adenovirus type 5." Journal of General Virology **36**(1): 59-74.

Grammel, D., M. Warmuth-Metz, A. O. von Bueren, M. Kool, T. Pietsch, H. A. Kretzschmar, D. H. Rowitch, S. Rutkowski, S. M. Pfister and U. Schüller (2012). "Sonic hedgehog-associated medulloblastoma arising from the cochlear nuclei of the brainstem." Acta Neuropathologica **123**(4): 601-614.

Grech-Sollars, M., D. E. Saunders, K. P. Phipps, J. D. Clayden and C. A. Clark (2012). "Survival analysis for apparent diffusion coefficient measures in children with embryonal brain tumours." Neuro-Oncology **14**(10): 1285-1293.

Hammerschmidt, M., A. Brook and A. P. McMahon (1997). "The world according to hedgehog." Trends in Genetics **13**(1): 14-21.

Harada, N., Y. Tamai, T. Ishikawa, B. Sauer, K. Takaku, M. Oshima and M. M. Taketo (1999). "Intestinal polyposis in mice with a dominant stable mutation of the beta-catenin gene." EMBO Journal **18**(21): 5931-5942.

He, T. C., A. B. Sparks, C. Rago, H. Hermeking, L. Zawel, L. T. da Costa, P. J. Morin, B. Vogelstein and K. W. Kinzler (1998). "Identification of c-MYC as a target of the APC pathway." Science **281**(5382): 1509-1512.

Heine, V. M. and D. H. Rowitch (2009). "Hedgehog signaling has a protective effect in glucocorticoid-induced mouse neonatal brain injury through an 11betaHSD2-dependent mechanism." Journal of Clinical Investigation **119**(2): 267-277.

Ingham, P. W. and A. P. McMahon (2001). "Hedgehog signaling in animal development: paradigms and principles." Genes and Development **15**(23): 3059-3087.

Ingham, P. W., Y. Nakano and C. Seger (2011). "Mechanisms and functions of Hedgehog signalling across the metazoa." Nat Rev Genet **12**(6): 393-406.

Ingham, P. W. and M. Placzek (2006). "Orchestrating ontogenesis: variations on a theme by sonic hedgehog." Nat Rev Genet **7**(11): 841-850.

Ingham, P. W., A. M. Taylor and Y. Nakano (1991). "Role of the Drosophila patched gene in positional signalling." Nature **353**(6340): 184-187.

Janda, C. Y., D. Waghray, A. M. Levin, C. Thomas and K. C. Garcia (2012). "Structural basis of Wnt recognition by Frizzled." Science **337**(6090): 59-64.

Jeong, J., J. Mao, T. Tenzen, A. H. Kottmann and A. P. McMahon (2004). "Hedgehog signaling in the neural crest cells regulates the patterning and growth of facial primordia." Genes and Development **18**(8): 937-951.

Jessell, T. M. (2000). "Neuronal specification in the spinal cord: inductive signals and transcriptional codes." Nat Rev Genet **1**(1): 20-29.

Juers, D. H., B. W. Matthews and R. E. Huber (2012). "LacZ beta-galactosidase: structure and function of an enzyme of historical and molecular biological importance." Protein Science **21**(12): 1792-1807.

Kim, C. H., T. Oda, M. Itoh, D. Jiang, K. B. Artinger, S. C. Chandrasekharappa, W. Driever and A. B. Chitnis (2000). "Repressor activity of Headless/Tcf3 is essential for vertebrate head formation." Nature **407**(6806): 913-916.

Kinzler, K. W., M. C. Nilbert, L. K. Su, B. Vogelstein, T. M. Bryan, D. B. Levy, K. J. Smith, A. C. Preisinger, P. Hedge, D. McKechnie and et al. (1991). "Identification of FAP locus genes from chromosome 5q21." Science **253**(5020): 661-665.

Kinzler, K. W. and B. Vogelstein (1996). "Lessons from hereditary colorectal cancer." Cell **87**(2): 159-170.

Klaus, A. and W. Birchmeier (2008). "Wnt signalling and its impact on development and cancer." Nature Reviews: Cancer **8**(5): 387-398.

Klein, P. S. and D. A. Melton (1996). "A molecular mechanism for the effect of lithium on development." Proceedings of the National Academy of Sciences of the United States of America **93**(16): 8455-8459.

Komiya, Y. and R. Habas (2008). "Wnt signal transduction pathways." Organogenesis **4**(2): 68-75.

Korinek, V., N. Barker, P. J. Morin, D. van Wichen, R. de Weger, K. W. Kinzler, B. Vogelstein and H. Clevers (1997). "Constitutive transcriptional activation by a beta-catenin-Tcf complex in APC-/- colon carcinoma." Science **275**(5307): 1784-1787.

Korshunov, A., M. Remke, M. Gessi, M. Ryzhova, T. Hielscher, H. Witt, V. Tobias, A. Buccoliero, I. Sardi, M. Gardiman, J. Bonnin, B. Scheithauer, A. Kulozik, O. Witt, S. Mork, A. von Deimling, O. Wiestler, F. Giangaspero, M. Rosenblum, T. Pietsch, P. Lichter and S. Pfister (2010). "Focal genomic amplification at 19q13.42 comprises a powerful diagnostic marker for embryonal tumors with ependymoblastic rosettes." Acta Neuropathologica **120**(2): 253-260.

Korshunov, A., M. Ryzhova, D. T. Jones, P. A. Northcott, P. van Sluis, R. Volckmann, J. Koster, R. Versteeg, C. Cowdrey, A. Perry, D. Picard, M. Rosenblum, F. Giangaspero, E. Aronica, U. Schüller, M. Hasselblatt, V. P. Collins, A. von Deimling, P. Lichter, A. Huang, S. M. Pfister and M. Kool (2012). "LIN28A immunoreactivity is a potent diagnostic marker of embryonal tumor with multilayered rosettes (ETMR)." Acta Neuropathologica **124**(6): 875-881.

Korshunov, A., D. Sturm, M. Ryzhova, V. Hovestadt, M. Gessi, D. T. Jones, M. Remke, P. Northcott, A. Perry, D. Picard, M. Rosenblum, M. Antonelli, E. Aronica, U. Schüller, M. Hasselblatt, A. Woehrer, O. Zheludkova, E. Kumirova, S. Puget, M. D. Taylor, F. Giangaspero, V. Peter Collins, A. von Deimling, P. Lichter, A. Huang, T. Pietsch, S. M. Pfister and M. Kool (2014). "Embryonal tumor with abundant neuropil and true rosettes (ETANTR), ependymoblastoma, and medulloepithelioma share molecular similarity and comprise a single clinicopathological entity." Acta Neuropathologica **128**(2): 279-289.

Lancaster, M. A., D. J. Gopal, J. Kim, S. N. Saleem, J. L. Silhavy, C. M. Louie, B. E. Thacker, Y. Williams, M. S. Zaki and J. G. Gleeson (2011). "Defective Wnt-dependent cerebellar midline fusion in a mouse model of Joubert syndrome." Nature Medicine **17**(6): 726-731.

Lauth, M. and R. Toftgard (2011). "Hedgehog signaling and pancreatic tumor development." Advances in Cancer Research **110**: 1-17.

Lepourcelet, M., Y. N. Chen, D. S. France, H. Wang, P. Crews, F. Petersen, C. Bruseo, A. W. Wood and R. A. Shivdasani (2004). "Small-molecule antagonists of the oncogenic Tcf/beta-catenin protein complex." Cancer Cell **5**(1): 91-102.

Li, M., K. F. Lee, Y. Lu, I. Clarke, D. Shih, C. Eberhart, V. P. Collins, T. Van Meter, D. Picard, L. Zhou, P. C. Boutros, P. Modena, M. L. Liang, S. W. Scherer, E. Bouffet, J. T. Rutka, S. L. Pomeroy, C. C. Lau, M. D. Taylor, A. Gajjar, P. B. Dirks, C. E. Hawkins and A. Huang (2009). "Frequent amplification of a chr19q13.41 microRNA polycistron in aggressive primitive neuroectodermal brain tumors." Cancer Cell **16**(6): 533-546.

Li, M. H., E. Bouffet, C. E. Hawkins, J. A. Squire and A. Huang (2005). "Molecular genetics of supratentorial primitive neuroectodermal tumors and pineoblastoma." Neurosurgical Focus **19**(5): E3.

Lorenz, A., M. Deutschmann, J. Ahlfeld, C. Prix, A. Koch, R. Smits, R. Fodde, H. A. Kretzschmar and U. Schüller (2011). "Severe alterations of cerebellar cortical development after constitutive activation of Wnt signaling in granule neuron precursors." Molecular and Cellular Biology **31**(16): 3326-3338.

Louis, D. N., H. Ohgaki, O. D. Wiestler, W. K. Cavenee, P. C. Burger, A. Jouvet, B. W. Scheithauer and P. Kleihues (2007). "The 2007 WHO classification of tumours of the central nervous system." Acta Neuropathologica **114**(2): 97-109.

Machold, R. and G. Fishell (2002). "Hedgehog patterns midbrain ARChitecture." Trends in Neurosciences **25**(1): 10-11.

Maes, W. and S. W. Van Gool (2011). "Experimental immunotherapy for malignant glioma: lessons from two decades of research in the GL261 model." Cancer Immunology, Immunotherapy **60**(2): 153-160.

Makoukji, J., M. Belle, D. Meffre, R. Stassart, J. Grenier, G. Shackleford, R. Fledrich, C. Fonte, J. Branchu, M. Goulard, C. de Waele, F. Charbonnier, M. W. Sereda, E. E. Baulieu, M. Schumacher, S. Bernard and C. Massaad (2012). "Lithium enhances remyelination of peripheral nerves." Proceedings of the National Academy of Sciences of the United States of America **109**(10): 3973-3978.

Mann, R. K. and P. A. Beachy (2004). "Novel lipid modifications of secreted protein signals." Annual Review of Biochemistry **73**: 891-923.

Mao, J., K. L. Ligon, E. Y. Rakhlin, S. P. Thayer, R. T. Bronson, D. Rowitch and A. P. McMahon (2006). "A novel somatic mouse model to survey tumorigenic potential applied to the Hedgehog pathway." Cancer Research **66**(20): 10171-10178.

Matei, V., S. Pauley, S. Kaing, D. Rowitch, K. W. Beisel, K. Morris, F. Feng, K. Jones, J. Lee and B. Fritzsch (2005). "Smaller inner ear sensory epithelia in Neurog1 null mice are related to earlier hair cell cycle exit." Developmental Dynamics **234**(3): 633-650.

Nanni, L., J. E. Ming, M. Bocian, K. Steinhaus, D. W. Bianchi, C. Die-Smulders, A. Giannotti, K. Imaizumi, K. L. Jones, M. D. Campo, R. A. Martin, P. Meinecke, M. E. Pierpont, N. H. Robin, I. D. Young, E. Roessler and M. Muenke (1999). "The mutational spectrum of the sonic hedgehog gene in holoprosencephaly: SHH mutations cause a significant proportion of autosomal dominant holoprosencephaly." Human Molecular Genetics **8**(13): 2479-2488.

Nehls, M., K. Luno, M. Schorpp, S. Krause, U. Matysiak-Scholze, C. M. Prokop, H. J. Hedrich and T. Boehm (1994). "A yeast artificial chromosome contig on mouse chromosome 11 encompassing the nu locus." European Journal of Immunology **24**(7): 1721-1723.

Niida, A., T. Hiroko, M. Kasai, Y. Furukawa, Y. Nakamura, Y. Suzuki, S. Sugano and T. Akiyama (2004). "DKK1, a negative regulator of Wnt signaling, is a target of the beta-catenin/TCF pathway." Oncogene **23**(52): 8520-8526.

Northcott, P. A., A. M. Dubuc, S. Pfister and M. D. Taylor (2012). "Molecular subgroups of medulloblastoma." Expert Review of Neurotherapeutics **12**(7): 871-884.

Nusse, R. and H. E. Varmus (1982). "Many tumors induced by the mouse mammary tumor virus contain a provirus integrated in the same region of the host genome." Cell **31**(1): 99-109.

O'Brien, W. T. and P. S. Klein (2009). "Validating GSK3 as an in vivo target of lithium action." Biochemical Society Transactions **37**(Pt 5): 1133-1138.

Oliver, T. G., T. A. Read, J. D. Kessler, A. Mehmeti, J. F. Wells, T. T. Huynh, S. M. Lin and R. J. Wechsler-Reya (2005). "Loss of patched and disruption of granule cell development in a pre-neoplastic stage of medulloblastoma." Development **132**(10): 2425-2439.

Pantelouris, E. M. and J. Hair (1970). "Thymus dysgenesis in nude (nu nu) mice." Journal of Embryology and Experimental Morphology **24**(3): 615-623.

Paulus, W. and P. Kleihues (2010). "Genetic profiling of CNS tumors extends histological classification." Acta Neuropathologica **120**(2): 269-270.

Picard, D., S. Miller, C. E. Hawkins, E. Bouffet, H. A. Rogers, T. S. Chan, S. K. Kim, Y. S. Ra, J. Fangusaro, A. Korshunov, H. Toledano, H. Nakamura, J. T. Hayden, J. Chan, L. Lafay-Cousin, P. Hu, X. Fan, K. M. Muraszko, S. L. Pomeroy, C. C. Lau, H. K. Ng, C. Jones, T. Van Meter, S. C. Clifford, C. Eberhart, A. Gajjar, S. M. Pfister, R. G. Grundy and A. Huang (2012). "Markers of survival and metastatic potential in childhood CNS primitive neuro-ectodermal brain tumours: an integrative genomic analysis." Lancet Oncology **13**(8): 838-848.

Pietsch, T., A. Waha, A. Koch, J. Kraus, S. Albrecht, J. Tonn, N. Sorensen, F. Berthold, B. Henk, N. Schmandt, H. K. Wolf, A. von Deimling, B. Wainwright, G. Chenevix-Trench, O. D. Wiestler and C. Wicking (1997). "Medulloblastomas of the desmoplastic variant carry mutations of the human homologue of Drosophila patched." Cancer Research **57**(11): 2085-2088.

Pignata, C., M. Fiore, V. Guzzetta, A. Castaldo, G. Sebastio, F. Porta and A. Guarino (1996). "Congenital Alopecia and nail dystrophy associated with severe functional T-cell immunodeficiency in two sibs." American Journal of Medical Genetics **65**(2): 167-170.

Pinson, K. I., J. Brennan, S. Monkley, B. J. Avery and W. C. Skarnes (2000). "An LDL-receptor-related protein mediates Wnt signalling in mice." Nature **407**(6803): 535-538.

Pizer, B. L., C. L. Weston, K. J. Robinson, D. W. Ellison, J. Ironside, F. Saran, L. S. Lashford, D. Tait, H. Lucraft, D. A. Walker, C. C. Bailey and R. E. Taylor (2006). "Analysis of patients with supratentorial primitive neuro-ectodermal tumours entered into the SIOP/UKCCSG PNET 3 study." European Journal of Cancer **42**(8): 1120-1128.

Popperl, H., C. Schmidt, V. Wilson, C. R. Hume, J. Dodd, R. Krumlauf and R. S. Beddington (1997). "Misexpression of Cwnt8C in the mouse induces an ectopic embryonic axis and causes a truncation of the anterior neuroectoderm." Development **124**(15): 2997-3005.

Pöschl, J., M. Bartels, J. Ohli, E. Bianchi, K. Kuteykin-Teplyakov, D. Grammel, J. Ahlfeld and U. Schüller (2014). "Wnt/β-catenin signaling inhibits the Shh pathway and impairs tumor growth in Shh-dependent medulloblastoma." Acta Neuropathologica **127**(4): 605-607.

Pöschl, J., D. Grammel, M. M. Dorostkar, H. A. Kretzschmar and U. Schüller (2013). "Constitutive activation of beta-catenin in neural progenitors results in disrupted proliferation and migration of neurons within the central nervous system." Developmental Biology **374**(2): 319-332.

Reed, K. R., V. S. Meniel, V. Marsh, A. Cole, O. J. Sansom and A. R. Clarke (2008). "A limited role for p53 in modulating the immediate phenotype of Apc loss in the intestine." BMC Cancer **8**: 162-162.

Remke, M., V. Ramaswamy and M. D. Taylor (2013). "Medulloblastoma molecular dissection: the way toward targeted therapy." Current Opinion in Oncology **25**(6): 674-681.

Ris, M. D., R. Packer, J. Goldwein, D. Jones-Wallace and J. M. Boyett (2001). "Intellectual outcome after reduced-dose radiation therapy plus adjuvant chemotherapy for medulloblastoma: a Children's Cancer Group study." Journal of Clinical Oncology **19**(15): 3470-3476.

Robbins, D. J., D. L. Fei and N. A. Riobo (2012). "The Hedgehog signal transduction network." Sci Signal **5**(246): re6.

Roussel, M. F. and M. E. Hatten (2011). "Cerebellum development and medulloblastoma." Current Topics in Developmental Biology **94**: 235-282.

Rudin, C. M., C. L. Hann, J. Laterra, R. L. Yauch, C. A. Callahan, L. Fu, T. Holcomb, J. Stinson, S. E. Gould, B. Coleman, P. M. LoRusso, D. D. Von Hoff, F. J. de Sauvage and J. A. Low (2009). "Treatment of medulloblastoma with hedgehog pathway inhibitor GDC-0449." New England Journal of Medicine **361**(12): 1173-1178.

Sasaki, H., Y. Nishizaki, C. Hui, M. Nakafuku and H. Kondoh (1999). "Regulation of Gli2 and Gli3 activities by an amino-terminal repression domain: implication of Gli2 and Gli3 as primary mediators of Shh signaling." Development **126**(17): 3915-3924.

Schlake, T. (2001). "The nude gene and the skin." Experimental Dermatology **10**(5): 293-304.

Schorpp, M., M. Hofmann, T. N. Dear and T. Boehm (1997). "Characterization of mouse and human nude genes." Immunogenetics **46**(6): 509-515.

Schüller, U., V. M. Heine, J. Mao, A. T. Kho, A. K. Dillon, Y. G. Han, E. Huillard, T. Sun, A. H. Ligon, Y. Qian, Q. Ma, A. Alvarez-Buylla, A. P. McMahon, D. H. Rowitch and K. L. Ligon (2008). "Acquisition of granule neuron precursor identity is a critical determinant of progenitor cell competence to form Shh-induced medulloblastoma." Cancer Cell **14**(2): 123-134.

Schüller, U., Q. Zhao, S. A. Godinho, V. M. Heine, R. H. Medema, D. Pellman and D. H. Rowitch (2007). "Forkhead transcription factor FoxM1 regulates mitotic entry and prevents spindle defects in cerebellar granule neuron precursors." Molecular and Cellular Biology **27**(23): 8259-8270.

Sekulic, A., M. R. Migden, A. E. Oro, L. Dirix, K. D. Lewis, J. D. Hainsworth, J. A. Solomon, S. Yoo, S. T. Arron, P. A. Friedlander, E. Marmur, C. M. Rudin, A. L. S. Chang, J. A. Low, H. M. Mackey, R. L. Yauch, R. A. Graham, J. C. Reddy and A. Hauschild (2012). "Efficacy and Safety of Vismodegib in Advanced Basal-Cell Carcinoma." New England Journal of Medicine **366**(23): 2171-2179.

Selvadurai, H. J. and J. O. Mason (2011). "Wnt/beta-catenin signalling is active in a highly dynamic pattern during development of the mouse cerebellum." PloS One **6**(8): e23012.

Sin-Chan, P. and A. Huang (2014). "DNMTs as potential therapeutic targets in high-risk pediatric embryonal brain tumors." Expert Opinion on Therapeutic Targets **18**(10): 1103-1107.

Smoll, N. R. (2012). "Relative survival of childhood and adult medulloblastomas and primitive neuroectodermal tumors (PNETs)." Cancer **118**(5): 1313-1322.

Stambolic, V., L. Ruel and J. R. Woodgett (1996). "Lithium inhibits glycogen synthase kinase-3 activity and mimics wingless signalling in intact cells." Current Biology **6**(12): 1664-1668.

Storosum, J. G., T. Wohlfarth, A. Schene, A. Elferink, B. J. Van Zwieten and W. v. d. Brink (2007). "Magnitude of effect of lithium in short-term efficacy studies of moderate to severe manic episode." Bipolar Disorders **9**(8): 793-798.

Taipale, J., J. K. Chen, M. K. Cooper, B. Wang, R. K. Mann, L. Milenkovic, M. P. Scott and P. A. Beachy (2000). "Effects of oncogenic mutations in Smoothened and Patched can be reversed by cyclopamine." Nature **406**(6799): 1005-1009.

Taipale, J., M. K. Cooper, T. Maiti and P. A. Beachy (2002). "Patched acts catalytically to suppress the activity of Smoothened." Nature **418**(6900): 892-897.

Tamai, K., X. Zeng, C. Liu, X. Zhang, Y. Harada, Z. Chang and X. He (2004). "A mechanism for Wnt coreceptor activation." Molecular Cell **13**(1): 149-156.

Tang, M., J. C. Villaescusa, S. X. Luo, C. Guitarte, S. Lei, Y. Miyamoto, M. M. Taketo, E. Arenas and E. J. Huang (2010). "Interactions of Wnt/beta-catenin signaling and sonic hedgehog regulate the neurogenesis of ventral midbrain dopamine neurons." Journal of Neuroscience **30**(27): 9280-9291.

Ten Berge, D., D. Kurek, T. Blauwkamp, W. Koole, A. Maas, E. Eroglu, R. K. Siu and R. Nusse (2011). "Embryonic stem cells require Wnt proteins to prevent differentiation to epiblast stem cells." Nature Cell Biology **13**(9): 1070-1075.

Thorne, R. N., A. D. Pearson, J. A. Nicoll, H. B. Coakham, A. Oakhill, M. G. Mott and N. K. Foreman (1994). "Decline in incidence of medulloblastoma in children." Cancer **74**(12): 3240-3244.

Timmermann, B., R. D. Kortmann, J. Kuhl, S. Rutkowski, C. Meisner, T. Pietsch, F. Deinlein, C. Urban, M. Warmuth-Metz and M. Bamberg (2006). "Role of radiotherapy in supratentorial primitive neuroectodermal tumor in young children: results of the German HIT-SKK87 and HIT-SKK92 trials." Journal of Clinical Oncology **24**(10): 1554-1560.

Vistica, D. T., P. Skehan, D. Scudiero, A. Monks, A. Pittman and M. R. Boyd (1991). "Tetrazolium-based assays for cellular viability: a critical examination of selected parameters affecting formazan production." Cancer Research **51**(10): 2515-2520.

Wechsler-Reya, R. J. and M. P. Scott (1999). "Control of neuronal precursor proliferation in the cerebellum by Sonic Hedgehog." Neuron **22**(1): 103-114.

Wesseling, P. (2014). "Embryonal tumor with multilayered rosettes (ETMR): signed, sealed, delivered." Acta Neuropathologica **128**(2): 305-308.

Willert, K., C. Y. Logan, A. Arora, M. Fish and R. Nusse (1999). "A Drosophila Axin homolog, Daxin, inhibits Wnt signaling." Development **126**(18): 4165-4173.

Wu, X., P. A. Northcott, A. Dubuc, A. J. Dupuy, D. J. Shih, H. Witt, S. Croul, E. Bouffet, D. W. Fults, C. G. Eberhart, L. Garzia, T. Van Meter, D. Zagzag, N. Jabado, J. Schwartzentruber, J. Majewski, T. E. Scheetz, S. M. Pfister, A. Korshunov, X. N. Li, S. W. Scherer, Y. J. Cho, K. Akagi, T. J. MacDonald, J. Koster, M. G. McCabe, A. L. Sarver, V. P. Collins, W. A. Weiss, D. A. Largaespada, L. S. Collier and M. D. Taylor (2012). "Clonal selection drives genetic divergence of metastatic medulloblastoma." Nature **482**(7386): 529-533.

Xie, J., M. Murone, S. M. Luoh, A. Ryan, Q. Gu, C. Zhang, J. M. Bonifas, C. W. Lam, M. Hynes, A. Goddard, A. Rosenthal, E. H. Epstein, Jr. and F. J. de Sauvage (1998). "Activating Smoothened mutations in sporadic basal-cell carcinoma." Nature **391**(6662): 90-92.

Yamaguchi, T. P., A. Bradley, A. P. McMahon and S. Jones (1999). "A Wnt5a pathway underlies outgrowth of multiple structures in the vertebrate embryo." Development **126**(6): 1211-1223.

Yan, D., M. Wiesmann, M. Rohan, V. Chan, A. B. Jefferson, L. Guo, D. Sakamoto, R. H. Caothien, J. H. Fuller, C. Reinhard, P. D. Garcia, F. M. Randazzo, J. Escobedo, W. J. Fantl and L. T. Williams (2001). "Elevated expression of axin2 and hnkd mRNA provides evidence that Wnt/beta -catenin signaling is activated in human colon tumors." Proceedings of the National Academy of Sciences of the United States of America **98**(26): 14973-14978.

Yu, W., K. McDonnell, M. M. Taketo and C. B. Bai (2008). "Wnt signaling determines ventral spinal cord cell fates in a time-dependent manner." Development **135**(22): 3687-3696.

Zhang, Z., P. Burnley, B. Coder and D. M. Su (2012). "Insights on FoxN1 biological significance and usages of the "nude" mouse in studies of T-lymphopoiesis." International Journal of Biological Sciences **8**(8): 1156-1167.

Zhuo, L., M. Theis, I. Alvarez-Maya, M. Brenner, K. Willecke and A. Messing (2001). "hGFAP-cre transgenic mice for manipulation of glial and neuronal function in vivo." genesis **31**(2): 85-94.

7. Acknowledgements

I want to sincerely thank my supervisors PD Dr. med. Ulrich Schüller and Dr. med. Julia Neumann for offering me the possibility to work on such a fascinating topic. They were extremely supportive and always dedicated me their time and attention, for which I am greatly thankful. Their influence played an essential role in the development of my own critical thinking on scientific subjects. Furthermore, I would like to thank the former director of the Zentrum für Neuropathologie und Prionforschung Prof. Dr. med. Dr. h.c. Hans Kretzschmar, who unfortunately passed away last year, as well as the acting director Prof. Dr. med. Armin Giese for giving me the opportunity to carry out my work at their institution. I am indebted to Silvia Occhionero, Michael Schmidt and Veronika Kaltenbrunn for outstanding technical support and to Dr. Gerda Mitteregger-Kretzschmar, Dr. Mehdi Shakarami and Dr. Julia Geyer for animal husbandry. Furthermore, I refer to Drs. Daniel Grammel, Felix Schmidt and Julia Ahlfeld and all the doctoral students in our lab for their advice and great technical support.

This thesis is dedicated to Davide, Anna, Jamal and all people suffering from embryonal brain tumors.

Eidesstattliche Versicherung

Bianchi, Edoardo

Name, Vorname

Ich erkläre hiermit an Eides statt,

dass ich die vorliegende Dissertation mit dem Thema

The role of the Sonic-hedgehog and Wnt/ β-Catenin pathways in medulloblastoma and in embryonal brain tumors with multi-layered rosettes

selbständig verfasst, mich außer der angegebenen keiner weiteren Hilfsmittel bedient und alle Erkenntnisse, die aus dem Schrifttum ganz oder annähernd übernommen sind, als solche kenntlich gemacht und nach ihrer Herkunft unter Bezeichnung der Fundstelle einzeln nachgewiesen habe.

Ich erkläre des Weiteren, dass die hier vorgelegte Dissertation nicht in gleicher oder in ähnlicher Form bei einer anderen Stelle zur Erlangung eines akademischen Grades eingereicht wurde.

Berlin, 24/7/2016

Ort, Datum

Unterschrift Doktorandin/Doktorand